Electroweak constraints on warped models with custodial symmetry

Marcela Carena,[1] Eduardo Pontón,[2] José Santiago,[1] and C. E. M. Wagner[3,4]
[1]*Fermi National Accelerator Laboratory, P.O. Box 500, Batavia, Illinois 60510, USA*
[2]*Department of Physics, Columbia University, 538 West 120th Street, New York, New York 10027, USA*
[3]*HEP Division, Argonne National Laboratory, 9700 Cass Avenue, Argonne, Illinois 60439, USA*
[4]*Enrico Fermi Institute and Kavli Institute for Cosmological Physics, University of Chicago, 5640 Ellis Avenue, Chicago, Illinois 60637, USA*
(Received 14 February 2007; published 28 August 2007)

It has been recently argued that realistic models with warped extra dimensions can have Kaluza-Klein particles accessible at the CERN Large Hadron Collider if a custodial symmetry, $SU(2)_V \times P_{LR}$, is used to protect the T parameter and the coupling of the left-handed bottom quark to the Z gauge boson. In this article we emphasize that such a symmetry implies that the loop corrections to both the T parameter and the $Zb_L\bar{b}_L$ coupling are calculable. In general, these corrections are correlated, can be sizable, and should be considered to determine the allowed parameter space region in models with warped extra dimensions and custodial symmetry, including Randall-Sundrum models with a fundamental Higgs, models of gauge-Higgs unification, and Higgsless models. As an example, we derive the constraints that arise on a representative model of gauge-Higgs unification from a global fit to the precision electroweak observables. A scan over the parameter space typically leads to a lower bound on the Kaluza-Klein excitations of the gauge bosons of about 2–3 TeV, depending on the configuration. In the fermionic sector one can have Kaluza-Klein excitations with masses of a few hundred GeV. We present the constraints on these light fermions from recent Tevatron searches, and explore interesting discovery channels at the LHC.

DOI: 10.1103/PhysRevD.76.035006 PACS numbers: 12.60.Cn, 04.50.+h, 12.15.Lk

I. INTRODUCTION

Models with warped extra dimensions [1] represent a very exciting alternative to more traditional extensions of the standard model (SM), like supersymmetry. These models provide not only a natural solution to the hierarchy problem, but also a very compelling theory of flavor, when fermions are allowed to propagate in the bulk [2]. The large hierarchies among the different fermion masses arise in a natural way, without inducing new sources of flavor violation for the first and second generation fermions. On the other hand, large flavor violation effects are predicted for the third generation fermions, most notably for the top quark [3]. It has been recently realized that an enlarged bulk gauge symmetry,

$$SU(2)_L \times SU(2)_R \times U(1)_X, \tag{1}$$

can act as a custodial symmetry that protects two of the most constraining observables from large tree-level corrections: the Peskin-Takeuchi [4] T parameter [5] and, if an extra discrete left-right symmetry P_{LR} is imposed, the anomalous $Zb_L\bar{b}_L$ coupling [6].[1] When the zero modes of the first two generations are localized far from the IR brane, so as to explain the low-energy flavor structure, an analysis of the electroweak (EW) precision data based on the oblique corrections parametrized by S and T, together with the heavy flavor asymmetries and branching ratios, takes into account the most important effects. Therefore, at tree level, the custodial protection of the T parameter and the $Zb_L\bar{b}_L$ coupling leaves the S parameter as the only relevant constraint.

However, as emphasized in [8], there are calculable one-loop corrections to the precision electroweak observables, which can be relevant and should be taken into account. In fact, for the choice of quantum numbers that lead to the custodial protection of the $Zb_L\bar{b}_L$ coupling, it was shown that the contribution of these loop corrections yields tight constraints on the parameters of these models, which in turn can have interesting implications for the spectrum of Kaluza-Klein (KK) states and their phenomenology.

In Ref. [8] we performed an analysis of the constraints from precision electroweak observables, including one-loop effects, for a specific model based on gauge-Higgs unification, when the light fermions are localized near the UV brane. We obtained a bound on the mass of the first level KK excitations of the gauge bosons of about 3–4 TeV, together with light KK quarks with masses of the order of a few hundred GeV, some of them with exotic electric charges. Since the S parameter yields one of the most relevant constraints in these models, one would like to investigate whether scenarios with the light generation fermions localized near the conformal point (flat wave functions for the zero modes), where the couplings of these fermions to the $SU(2)_L$ KK modes are suppressed, can lead to a better fit [9]. Generically, however, an analysis based on the oblique approximation is not sufficient in this region, since the couplings of fermions to $SU(2)_R$ gauge bosons tend to induce anomalous, nonuniversal couplings to the W and Z gauge bosons.

It is important to emphasize that, due to the custodial symmetry, the corrections to the T parameter and the

[1]See [7] for a possible alternative to the custodial protection of the $Zb_L\bar{b}_L$ coupling.

$Zb_L\bar{b}_L$ vertex cannot receive contributions from higher-dimension 5D operators suppressed by a low cutoff scale and are, therefore, calculable. In addition, in any given model these two quantities satisfy a definite correlation which, in general, may be understood in terms of the contribution of the lightest KK modes. The potentially large loop corrections to the T parameter and the $Zb_L\bar{b}_L$ coupling, as well as the effects of the associated correlations, must be considered in any model that makes use of the custodial symmetry. This includes models of gauge-Higgs unification [10–12] and models with a fundamental Higgs or even without a Higgs [13].

In this work, we present the results of a global fit to all relevant EW precision observables, taking into account the correlations among them as well as possible nonuniversal effects, in a particular setting. We have chosen to test these ideas in the context of gauge-Higgs unification scenarios, which we find particularly well motivated theoretically since they address the little hierarchy problem present in Randall-Sundrum models with a fundamental Higgs. In addition, this framework naturally leads to light KK fermion states, often with exotic charges, which makes these scenarios quite interesting from a phenomenological point of view.

The outline of the paper is as follows. We introduce the model in Sec. II and discuss its main effects on EW observables in Sec. III. The results of the global fit are reported in Sec. IV and we discuss some simple variations in Sec. V. In Sec. VI we present an interesting example which allows for light KK fermions for the three generations within the reach of present and near future colliders. We discuss the bounds from EW precision observables in combination with those from direct searches at the Tevatron. We also discuss interesting search channels at the CERN LHC. Finally we conclude in Sec. VII. Some technical results are given in the Appendix.

II. A MODEL OF GAUGE-HIGGS UNIFICATION

Our setup is a five-dimensional model in a warped background,

$$ds^2 = e^{-2ky}\eta_{\mu\nu}dx^\mu dx^\nu - dy^2, \tag{2}$$

where $0 \le y \le L$. The bulk gauge symmetry is $SO(5) \times U(1)_X$, broken by boundary conditions to $SU(2)_L \times SU(2)_R \times U(1)_X$ on the IR brane ($y = L$), and to the standard model $SU(2)_L \times U(1)_Y$ gauge group on the UV brane ($y = 0$) [12]. The $U(1)_X$ charges are adjusted so as to recover the correct hypercharges, where $Y/2 = T_R^3 + Q_X$ with T_R^3 the third $SU(2)_R$ generator and Q_X the $U(1)_X$ charge. The fifth component of the gauge fields in $SO(5)/SU(2)_L \times SU(2)_R$ has a (four-dimensional scalar) zero mode with the quantum numbers of the Higgs boson. This zero mode has a nontrivial profile in the extra dimension [11],

$$A_5^{\hat{a}}(x, y) = A_5^{\hat{a}(0)}(x) f_H(y) + \ldots, \tag{3}$$

where $\hat{a}$ labels the generators of $SO(5)/SU(2)_L \times SU(2)_R$ and is exponentially localized towards the IR brane,

$$f_H(y) = \sqrt{\frac{2k}{e^{2kL} - 1}} e^{2ky}, \tag{4}$$

hence giving a solution to the hierarchy problem. The dots in Eq. (3) stand for massive KK modes that are eaten by the corresponding KK gauge fields.

The SM fermions are embedded in full representations of the bulk gauge group. The presence of the $SU(2)_R$ subgroup of the full bulk gauge symmetry ensures the custodial protection of the T parameter [5]. In order to have a custodial protection of the $Zb_L\bar{b}_L$ coupling, the choice $T_R^3(b_L) = T_L^3(b_L)$ has to be enforced [6]. An economical choice is to let the SM $SU(2)_L$ top-bottom doublet arise from a $\mathbf{5}_{2/3}$ of $SO(5) \times U(1)_X$, where the subscript refers to the $U(1)_X$ charge. As discussed in [8], putting the SM $SU(2)_L$ singlet top in the same $SO(5)$ multiplet as the doublet, without further mixing, is disfavored since, for the correct value of the top-quark mass, this leads to a large negative contribution to the T parameter at one loop. Hence we let the right-handed (RH) top quark arise from a second $\mathbf{5}_{2/3}$ of $SO(5) \times U(1)_X$. The right-handed bottom quark can come from a $\mathbf{10}_{2/3}$ that allows us to write the bottom Yukawa coupling. For simplicity, and because it allows the generation of the Cabibbo-Kobayashi-Maskawa (CKM) mixing matrix, we make the same choice for the first two quark generations. We therefore introduce in the quark sector three $SO(5)$ multiplets per generation as follows:

$$\begin{aligned}
\xi_{1L}^i \sim Q_{1L}^i &= \begin{pmatrix} \chi_{1L}^{u_i}(-,+) & q_L^{u_i}(+,+) \\ \chi_{1L}^{d_i}(-,+) & q_L^{d_i}(+,+) \end{pmatrix} \oplus u_L'^i(-,+), \\
\xi_{2R}^i \sim Q_{2R}^i &= \begin{pmatrix} \chi_{2R}^{u_i}(+,-) & q_R'^{u_i}(+,-) \\ \chi_{2R}^{d_i}(+,-) & q_R'^{d_i}(+,-) \end{pmatrix} \oplus u_R^i(+,+), \\
\xi_{3R}^i \sim T_{1R}^i &= \begin{pmatrix} \psi_R'^i(-,+) \\ U_R'^i(-,+) \\ D_R'^i(-,+) \end{pmatrix} \oplus T_{2R}^i \\
&= \begin{pmatrix} \psi_R''^i(-,+) \\ U_R''^i(-,+) \\ D_R^i(+,+) \end{pmatrix} \oplus Q_{3R}^i \\
&= \begin{pmatrix} \chi_{3R}^{u_i}(-,+) & q_R''^{u_i}(-,+) \\ \chi_{3R}^{d_i}(-,+) & q_R''^{d_i}(-,+) \end{pmatrix},
\end{aligned} \tag{5}$$

where we show the decomposition under $SU(2)_L \times SU(2)_R$. The Q^i's are bidoublets of $SU(2)_L \times SU(2)_R$, with $SU(2)_L$ acting vertically and $SU(2)_R$ acting horizontally. The T_1^i's and T_2^i's transform as $(\mathbf{3}, \mathbf{1})$ and $(\mathbf{1}, \mathbf{3})$ under $SU(2)_L \times SU(2)_R$, respectively, while u^i and u'^i are

$SU(2)_L \times SU(2)_R$ singlets. The superscripts, $i = 1, 2, 3$, label the three generations.

We also show the boundary conditions on the indicated 4D chirality, where $-$ stands for Dirichlet boundary conditions. The $+$ stands for a linear combination of Neumann and Dirichlet boundary conditions, which is determined via the fermion bulk equations of motion from the Dirichlet boundary condition obeyed by the opposite chirality. This ensures the consistency of the boundary conditions. In the absence of mixing among multiplets satisfying different boundary conditions, the SM fermions arise as the zero modes of the fields obeying $(+, +)$ boundary conditions. The remaining boundary conditions are chosen so that $SU(2)_L \times SU(2)_R$ is preserved on the IR brane, and so that mass mixing terms, necessary to obtain the SM fermion masses after EW symmetry breaking, can be written on the IR brane. It is possible to flip the boundary conditions on Q^i_{2R}, consistently with these requirements, and we will comment on such a possibility in later sections.

As for the leptons, one option is to embed the SM $SU(2)_L$ lepton doublets into the $\mathbf{5}_0$ representation of $SO(5) \times U(1)_X$ and the $SU(2)_L$ charged lepton singlets in a $\mathbf{10}_0$ representation. Right-handed neutrinos may come from the $SU(2)_L \times SU(2)_R$ singlet in the $\mathbf{5}_0$ representation, or from a different $\mathbf{5}_0$ representation, as in the quark sector. The boundary conditions may then be chosen in analogy with those in Eq. (5). A second possibility is that the leptons, unlike the quarks, arise from the four-dimensional spinorial representation of $SO(5)$, so that the SM lepton doublets transform as $(\mathbf{2}, \mathbf{1})$ under $SU(2)_L \times SU(2)_R$, while the SM lepton singlets transform as $(\mathbf{1}, \mathbf{2})$.

As remarked above, the zero-mode fermions can acquire EW symmetry breaking masses through mixing effects. The most general $SU(2)_L \times SU(2)_R \times U(1)_X$ invariant mass Lagrangian at the IR brane—compatible with the boundary conditions—is, in the quark sector,

$$\mathcal{L}_m = \delta(y - L)[\bar{u}'_L M_u u_R + \bar{Q}_{1L} M_d Q_{3R} + \bar{Q}_{2L} M_{ud} Q_{3R} + \text{H.c.}], \tag{6}$$

where M_u, M_d, and M_{ud} are dimensionless 3×3 matrices, and a matrix notation is employed.

III. EFFECTS ON ELECTROWEAK OBSERVABLES

In order to study the effects that the KK excitations of bulk fermions and gauge bosons have on EW observables, we compute the effective Lagrangian that results after integrating them out at tree level, keeping the leading corrections with operators of dimension six. As was mentioned in the Introduction, some one-loop corrections are also important and will be included on top of the tree-level effects. In fact, in models with custodial protection of the $Zb_L\bar{b}_L$ coupling, some of the KK fermions become considerably lighter than the KK gauge bosons and can give relevant loop-level effects as a result of their strong mixing with the top quark. The loop contributions to the EW observables coming from the gauge boson KK excitations are suppressed due to their larger masses, as well as to the fact that they couple via the EW gauge couplings, which are smaller than the top Yukawa coupling. Thus we expect their one-loop effects on EW observables to be subleading, and we neglect them.

A. Tree-level effective Lagrangian

In this section, we compute the effective Lagrangian up to dimension-six operators, obtained when the heavy physics in the models discussed in the previous section is integrated out at tree level. We will express the effective Lagrangian in the basis of [14] where the dimension-six operators are still $SU(2)_L \times U(1)_Y$ invariant. The procedure is the following. We integrate out the heavy physics in an explicitly $SU(2)_L \times U(1)_Y$ invariant way and then use the SM equations of motion if necessary to write the resulting operators in the basis of [14]. Only a subset of the 81 operators in that basis is relevant for EW precision observables, as discussed in [15]. At the order we are considering, we can integrate out independently each type of heavy physics. The effective Lagrangian in the basis of [14] after integrating out the heavy gauge bosons reads

$$\begin{aligned}\Delta\mathcal{L}_6 = {} & \alpha_h \mathcal{O}_h + \alpha^t_{hl}\mathcal{O}^t_{hl} + \alpha^t_{hq}\mathcal{O}^t_{hq} + \alpha^s_{hl}\mathcal{O}^s_{hl} + \alpha^s_{hq}\mathcal{O}^s_{hq} \\ & + \alpha_{hu}\mathcal{O}_{hu} + \alpha_{hd}\mathcal{O}_{hd} + \alpha_{he}\mathcal{O}_{he} + \alpha^t_{ll}\mathcal{O}^t_{ll} \\ & + \alpha^t_{lq}\mathcal{O}^t_{lq} + \alpha^s_{ll}\mathcal{O}^s_{ll} + \alpha^s_{lq}\mathcal{O}^s_{lq} + \alpha_{le}\mathcal{O}_{le} \\ & + \alpha_{qe}\mathcal{O}_{qe} + \alpha_{lu}\mathcal{O}_{lu} + \alpha_{ld}\mathcal{O}_{ld} + \alpha_{ee}\mathcal{O}_{ee} \\ & + \alpha_{eu}\mathcal{O}_{eu} + \alpha_{ed}\mathcal{O}_{ed} + \ldots,\end{aligned} \tag{7}$$

where the dots represent other operators that are irrelevant for the analysis of EW observables. Here h stands for the SM Higgs, q and l refer to the $SU(2)_L$ doublet quark and leptons, and u, d, e refer to the SM $SU(2)_L$ quark and lepton singlets. The list of the dimension-six operators generated in our model is as follows:

(i) Oblique operators

$$\mathcal{O}_h = |h^\dagger D_\mu h|^2. \tag{8}$$

(ii) Two-fermion operators

$$\begin{aligned}\mathcal{O}^s_{hl} &= \mathrm{i}(h^\dagger D_\mu h)(\bar{l}\gamma^\mu l) + \text{H.c.}, \\ \mathcal{O}^t_{hl} &= \mathrm{i}(h^\dagger \sigma^a D_\mu h)(\bar{l}\gamma^\mu \sigma^a l) + \text{H.c.}, \\ \mathcal{O}^s_{hq} &= \mathrm{i}(h^\dagger D_\mu h)(\bar{q}\gamma^\mu q) + \text{H.c.}, \\ \mathcal{O}^t_{hq} &= \mathrm{i}(h^\dagger \sigma^a D_\mu h)(\bar{q}\gamma^\mu \sigma^a q) + \text{H.c.}, \\ \mathcal{O}_{hd} &= \mathrm{i}(h^\dagger D_\mu h)(\bar{d}\gamma^\mu d) + \text{H.c.}, \\ \mathcal{O}_{hu} &= \mathrm{i}(h^\dagger D_\mu h)(\bar{u}\gamma^\mu u) + \text{H.c.}, \\ \mathcal{O}_{he} &= \mathrm{i}(h^\dagger D_\mu h)(\bar{e}\gamma^\mu e) + \text{H.c.}\end{aligned} \tag{9}$$

(iii) Four-fermion operators

$$\begin{aligned}
\mathcal{O}^{s}_{ll} &= \tfrac{1}{2}(\bar{l}\gamma^{\mu}l)(\bar{l}\gamma_{\mu}l),\\
\mathcal{O}^{t}_{ll} &= \tfrac{1}{2}(\bar{l}\gamma^{\mu}\sigma^{a}l)(\bar{l}\gamma_{\mu}\sigma^{a}l),\\
\mathcal{O}^{s}_{lq} &= (\bar{l}\gamma^{\mu}l)(\bar{q}\gamma_{\mu}q),\\
\mathcal{O}^{t}_{lq} &= (\bar{l}\gamma^{\mu}\sigma^{a}l)(\bar{q}\gamma_{\mu}\sigma^{a}q),\\
\mathcal{O}_{le} &= (\bar{l}\gamma^{\mu}l)(\bar{e}\gamma_{\mu}e),\\
\mathcal{O}_{qe} &= (\bar{q}\gamma^{\mu}q)(\bar{e}\gamma_{\mu}e),\\
\mathcal{O}_{lu} &= (\bar{l}\gamma^{\mu}l)(\bar{u}\gamma_{\mu}u),\\
\mathcal{O}_{ld} &= (\bar{l}\gamma^{\mu}l)(\bar{d}\gamma_{\mu}d),\\
\mathcal{O}_{ee} &= \tfrac{1}{2}(\bar{e}\gamma^{\mu}e)(\bar{e}\gamma_{\mu}e),\\
\mathcal{O}_{eu} &= (\bar{e}\gamma^{\mu}e)(\bar{u}\gamma_{\mu}u),\\
\mathcal{O}_{ed} &= (\bar{e}\gamma^{\mu}e)(\bar{d}\gamma_{\mu}d).
\end{aligned} \tag{10}$$

The coefficients α_i encode the dependence on the different parameters of our model, and their explicit form is given in the Appendix.

The heavy fermions can be integrated out in a similar fashion [16]. However, their effects are typically negligible for all the SM fermions except for the top quark [17], whose couplings are irrelevant for the EW precision observables (except for one-loop corrections [18] that will be considered in the next subsection). We have nevertheless included all these effects numerically.[2]

The operator $\mathcal{O}_h$ gives a direct contribution to the T parameter,

$$T = -\frac{4\pi v^2}{e^2}\alpha_h = -\frac{4\pi v^2}{c^2}[\delta^2_{++} - \delta^2_{-+}], \tag{11}$$

where α_h is the coefficient of the corresponding operator as given in the Appendix, e is the positron charge, c is the cosine of the weak mixing angle, $v = 174$ GeV is the Higgs vacuum expectation value (vev), and δ^2_{++} and δ^2_{-+} are functions depending on the Higgs and KK gauge boson wave functions, as defined in Eq. (A18). The (partial) cancellation between δ^2_{++} and δ^2_{-+} in the tree-level contribution to the T parameter of Eq. (11) is a consequence of the custodial symmetry. Also note that the S parameter, generated by the operator

$$\alpha_{WB}\mathcal{O}_{WB} = \alpha_{WB}(h^{\dagger}\sigma^{a}h)W^{a}_{\mu\nu}B^{\mu\nu}, \tag{12}$$

where $S = (32\pi sc/e^2)v^2\alpha_{WB}$, is not induced at tree level in our model.[3]

B. Relevant one-loop effects

Although higher-dimensional models are nonrenormalizable and many observables receive contributions from higher-dimension operators whose coefficients can only be determined by an unspecified UV completion, it is noteworthy that some of the low-energy observables are actually insensitive to the UV physics. This is the case of the Peskin-Takeuchi T parameter and of the $Zb_L\bar{b}_L$ coupling in models with custodial symmetry and the quantum numbers used in this paper. In particular, loop contributions to these parameters are dominated by the KK scale. This follows simply from the fact that the assumed symmetries [$SU(2)_L \times SU(2)_R$ with a discrete symmetry exchanging L with R] and quantum number assignments do not allow for local 5D counterterms that can contribute to these observables [5]. Note, however, that one can write operators that contribute to the $Zt_L\bar{t}_L$ coupling. Although these symmetries are broken by the boundary conditions at the UV brane, such breaking is nonlocal and effectively leads to finite contributions to the T parameter and the $Zb_L\bar{b}_L$ coupling at loop level.[4]

At one-loop order, the breaking of the custodial symmetry that is induced by the breaking of the $SU(2)_R$ factor due to the boundary conditions on the UV brane leads to nonvanishing contributions to the T parameter (as well as to the $Zb_L\bar{b}_L$ coupling). There are several diagrams that contribute, as first discussed in [5]. Of these, the ones giving rise to the largest effects are those involving the KK excitations of the top quark. Notice that these fermion contributions depend on various localization parameters in the fermion sector. One can also distinguish between those diagrams involving insertions of the Higgs vev in the fermion loop (similar to the top contribution to T in the SM) and those with Higgs vev insertions on the external gauge lines. The latter ones can lead to a nonvanishing contribution to T due to the $SU(2)_R$ breaking on the UV brane. Specifically, the mass splittings and different wave functions of the fermions within a given $SU(2)_R$ multiplet give a contribution to T through the self-polarization diagram for the $SU(2)_R$ gauge fields. Such effects vanish in the limit that the mass splittings and the difference in gauge

[2]There are potentially large tree-level mixing effects for the bottom quark as well [12], which *do* affect the EW precision observable fit. Such effects are, however, negligible with the current choice of quantum numbers and boundary conditions.

[3]Note that this is not in contradiction with previous claims that a moderate S parameter is generated in these models. This contribution to the S parameter comes from a field redefinition that absorbs a global shift in the gauge couplings of the light fermions into the oblique S parameter. Here we do not do that field redefinition, as the shift in the couplings is automatically included in the global fit.

[4]One can write counterterms that contribute to the T parameter on the UV brane, where the symmetry is reduced to that of the standard model. However, such effects are suppressed by the Planck scale, and also by the exponentially small Higgs wave function.

couplings of the fermions to the KK $SU(2)_R$ gauge fields tend to zero (notice that even in this limit the couplings of the L and R fermion chiralities are different, since we are considering the self-energies of KK gauge fields). We have estimated such effects by considering the contributions from the lowest lying KK fermion states, but summing over all gauge KK modes, and we find that their contribution is subdominant compared to the ones with Higgs insertions in the fermion loop.[5]

A second class of diagrams that contribute to the T parameter involve gauge fields in the loop, both with Higgs vev insertions in the loop and on the external legs. Note that such contributions do not depend on model parameters as do the ones arising from KK fermion loops. The nonvanishing contribution to T arises as a result of the mass splittings and difference in couplings between $SU(2)_L$ and $SU(2)_R$ gauge bosons. However, it is easy to see that the massive spectrum and couplings associated with $(+,+)$ versus $(-,+)$ boundary conditions are numerically very similar (they agree at the percent level). Thus, we expect the custodial cancellations to be very strong and that the effects of gauge bosons will give a small contribution to T compared to those arising from loops of fermions, which can easily have larger mass splittings. It would be interesting to verify this expectation through an explicit computation. Finally, also notice that in our gauge-Higgs unification scenario based on an $SO(5)$ gauge symmetry there are additional gauge fields corresponding to the $SO(5)/SO(4)$ generators. These transform as bidoublets of the $SU(2)_L \times SU(2)_R$ subgroup and have boundary conditions that respect the custodial symmetry. Therefore, they cannot give a contribution to T by themselves. They could give a contribution via electroweak symmetry breaking (EWSB) mixing effects with the $SU(2)_R$ gauge bosons, but again we expect strong cancellations with the corresponding diagrams involving $SU(2)_L$ KK gauge bosons. Therefore, we will neglect all pure gauge contributions to the T parameter in what follows.

The detailed computation of the leading one-loop contributions to the T parameter, i.e. those arising from the KK excitations of the top quark (with EWSB mass splittings), was first performed in [8]. The important observation made in that work is that the presence of bidoublets, necessary to protect the tree-level contribution to the $Zb_L\bar{b}_L$ coupling, typically induces a negative T parameter at one loop. There are also contributions from the KK excitations of the $SU(2)_L \times SU(2)_R$ singlets that can alter this result, provided these singlets are relatively light and mix sufficiently strongly with the top quark. In this case, a positive T might be obtained, but then the one-loop contributions to the $Zb_L\bar{b}_L$ coupling become sizable and therefore relevant for the EW fit.

The main one-loop effects, due to heavy vectorlike fermions that mix strongly with the top, can be computed by generalizing the results in Refs. [19,20]. We give the detailed formulas in the Appendix, which can be easily evaluated numerically. The largest contributions arise from the KK excitations that couple via the top Yukawa coupling. In the case of the T parameter, the quantitative features can be understood from the following types of contributions:

(i) A negative contribution to T from the lightest bidoublet excitations that violate the custodial symmetry via the boundary conditions, Q_1^3 in the notation of Eq. (5). The largest of these arise from EWSB mass mixing with the right-handed top quark.

(ii) A positive contribution to T from the EWSB mass mixing of the lightest $SU(2)_L \times SU(2)_R$ singlet KK excitations, u'^3 in the notation of Eq. (5), with the left-handed (LH) top quark or its KK excitations in the bidoublet, Q_1^3 (which breaks the custodial symmetry as mentioned in the previous item).

In Ref. [8] we also gave approximate analytic formulas for the above contributions. The expressions for the bidoublet are somewhat complicated, but the negative contribution arises [in the notation of Eq. (5)] from the first KK mode of the $(\chi_1^{u_3}, \chi_1^{d_3})$ $SU(2)_L$ doublet, which is lighter and couples more strongly to the Higgs than the lightest KK mode of the $(q_1^{u_3}, q_1^{d_3})$ $SU(2)_L$ doublet (which gives a partially compensating positive contribution). Notice that the contribution due to the Q_2^3 bidoublet is extremely small, even when these modes are very light, since the custodial symmetry is preserved by their boundary conditions. They can give a nonvanishing contribution to T only from mixing with other bidoublets that violate the custodial symmetry. Our choice for the boundary conditions of Q_2^3 is motivated by the desire to forbid a localized mixing mass term between Q_1^3 and Q_2^3, which would make the $(\chi_1^{u_3}, \chi_1^{d_3})$ KK modes very light and their contribution to the T parameter large and negative (which as we will review below is disfavored by the EW precision data. See also Ref. [8] for further details). In the region of parameter space favored by the EW precision data, the boundary conditions for Q_2^3 result in their KK excitations easily being in the few hundred GeV range, and present a very interesting phenomenology (see Sec. VI). It is in the above sense that we regard very light bidoublets as a rather well-motivated signature of the scenarios we are studying.

The positive contribution to T from the EWSB mass mixing of u'^3 with the left-handed top, mentioned above, is simply given by

[5]The precise evaluation of the diagrams with Higgs vev insertions in the external gauge lines is delicate since the contribution to T is finite only after renormalization of the $SU(2)_R$ gauge coupling [or the SO(5) gauge coupling in the model of Sec. II]. We have assumed that the dominant contribution comes from the lowest lying fermion states, subtracted by hand the divergence from the corresponding 4D momentum integral, and taken the renormalization scale of the order of the KK fermion masses appearing in the loop.

$$\Delta T = T_{\rm top}\frac{2m^2_{q^t_0,t}}{M_t^2}\left(\ln\frac{M_t^2}{m^2_{\rm top}} - 1 + \frac{m^2_{q^t_0,t}}{2m^2_{\rm top}}\right), \qquad (13)$$

where $T_{\rm top}$ is the SM contribution from the top quark, with mass $m_{\rm top}$, M_t is the KK mass of u'^3, and $m_{q^t_0,t}$ is the EW symmetry breaking mass mixing the lightest singlet with the SM (t, b) doublet. There are also terms that arise from the mixing between the first KK modes of the third generation Q_1^3 and u'^3, which can be relevant.

It is important that the dominant fermion loop contributions to the $Zb_L\bar{b}_L$ vertex arise from the same set of states as discussed above. The contributions coming from EWSB mass mixing of the singlet, u'^3, with the left-handed top quark are

$$\delta g^s_{b_L} = \frac{\alpha}{16\pi s^2 M_W^2}\frac{m^4_{q^t_0,t}}{M_t^2}\left[1 + 2\frac{m^2_{\rm top}}{m^2_{q^t_0,t}}\left(\ln\left(\frac{M_t^2}{m^2_{\rm top}}\right) - 1\right)\right], \qquad (14)$$

while those coming from Q_1^3 (mixing with the right-handed top quark through the Higgs vev) are

$$\delta g^q_{b_L} + \delta g^\chi_{b_L} = \frac{\alpha}{32\pi s^2 M_W^2} m^2_{\rm top}\left[\frac{m^2_{q^t,t}}{M_q^2}\ln\left(\frac{M_q^2}{m^2_{\rm top}}\right) - \frac{m^2_{\chi^d,t}}{M_\chi^2}\ln\left(\frac{M_\chi^2}{m^2_{\rm top}}\right)\right]. \qquad (15)$$

Here M_t, M_q, and M_χ are the KK masses of u'^3, $q_1^{u_3}$, and $\chi_1^{d_3}$, respectively, while $m_{q^t,t}$ and $m_{\chi^d,t}$ are the EW breaking masses that mix the right-handed top with the lightest KK modes of the two bidoublet components $q_1^{u_3}$ and $\chi_1^{d_3}$, respectively. Also, M_W is the W mass, α is the fine structure constant, and s is the sine of the weak mixing angle. There are additional contributions from the mixing between bidoublet and singlet KK modes, but we do not give the analytic expressions here since they are somewhat complicated. The dominant contribution arises from the singlet, but the mixing terms can also give a relevant effect.

One may also worry about the contributions to the $Zb_L\bar{b}_L$ vertex involving KK gauge fields [the results given in Eqs. (14) and (15) involve the W in the loop]. However, due to the high degeneracy between $SU(2)_L$ and $SU(2)_R$ gauge KK modes, these give a very small effect, which we neglect.

It should be noted that, although the above contributions to the T parameter and the $Zb_L\bar{b}_L$ depend on several mass and mixing parameters, within the context of an extra dimensional theory all of these are highly correlated by the shape of the wave functions. As an example, we show in Fig. 1 the correlation between the one-loop contributions to T and the $Zb_L\bar{b}_L$ vertex in the gauge-Higgs unification scenario based on the $SO(5)\times U(1)_X$ gauge symmetry, and with the fermion content given in Eq. (5). In particular, we see that, in the region where T becomes positive, the one-loop contribution to the $Zb_L\bar{b}_L$ vertex increases and cannot be neglected in the EW fit. In the figure, we did not include the tree-level contributions to the T parameter from gauge KK mode exchange, which are subdominant.

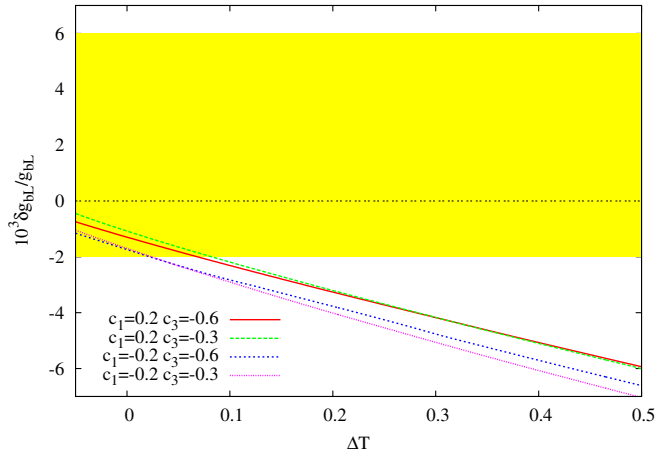

FIG. 1 (color online). Correlation between the one-loop contributions to the T parameter, denoted by ΔT, and the one-loop contributions to $\delta g_{b_L}/g_{b_L}$ in the model of Eq. (5). We show representative curves for a few values of the left-handed top-quark localization parameter c_1 and the bottom quark localization parameter c_3, as the right-handed top localization parameter c_2 is varied. We take the mass of the first KK excitation of the $SU(2)_L$ gauge bosons $m_1^{\rm gauge} = 3.75$ TeV. The band corresponds to the 2σ bound on $\delta g_{bL}/g_{bL}$, assuming no large corrections to the $Zb_R\bar{b}_R$ coupling.

Given the importance of these one-loop corrections, we have formally added them to the effective Lagrangian at the same level as the tree-level corrections computed in the previous section.[6] This is done by simply adding the corresponding results of Eqs. (A25)–(A30) to the coefficients of the operators $\mathcal{O}_h$ and $\mathcal{O}^t_{hQ}$ (here Q represents the doublet of the third generation).

We have also computed the one-loop fermion contributions to the S parameter [see Eq. (A26), as well as Ref. [8]]. Based on power counting, the corresponding contribution is expected to be dominated by the KK scale, and indeed one finds that at one loop the sum over KK modes converges relatively fast, although not as fast as in the case of the T parameter and the $Zb\bar{b}$ vertex.[7] In the region of parameter space we are interested, the corresponding contribution to S is not negligible, and we include it as a contribution to the operator $\mathcal{O}_{WB}$ defined in Eq. (12). We

[6]Note that the tree-level corrections arise from the gauge sector. Since the KK gauge bosons are heavier than the KK fermions, their tree-level effects can be comparable to the fermion one-loop effects. We expect higher-order loop corrections to be subleading, so they can be neglected.

[7]At higher-loop orders, the S parameter is UV sensitive, but assuming the validity of naive dimensional analysis (NDA) [21,22], such contributions are parametrically suppressed compared to both the tree- and one-loop contributions.

take this as a reasonable estimate of the total contribution to S in the models under discussion, but one should keep in mind that there are additional contributions from gauge loops that have not been computed and could be of comparable size. Also, there could be additional UV contributions to S that, at least in principle, could have a significant impact. Note that, when the light fermions are localized far from the IR brane, the universal shift in their couplings to the gauge bosons can be reabsorbed as an additional tree-level contribution to the S parameter. Since the tree- and loop-level contributions to the S parameter have the same sign, it is natural to assume that there are no particular cancellations when the effects of the physics above the UV cutoff are included. In particular, the S parameter is positive, thus disfavoring the regions of parameter space that lead to a negative T parameter [23].

IV. GLOBAL FIT TO ELECTROWEAK PRECISION OBSERVABLES

Having computed the leading corrections to the effective Lagrangian in the model of interest, we can compute the χ^2 function, defined by

$$\chi^2(\alpha_i) = \chi^2_{\text{min}} + (\alpha_i - \hat{\alpha}_i)\mathcal{M}_{ij}(\alpha_j - \hat{\alpha}_j), \qquad (16)$$

where the α_i's, as defined by Eq. (7), depend on the fundamental parameters of the model: localization parameters for each 5D fermion multiplet, c_{ξ_i}; localized fermion mass mixing parameters, M_u, M_d, and M_{ud}, as defined in Eq. (6); the gauge couplings, g_5 and g_{5X}; and the overall scale of the new physics, which we take as $\tilde{k} = ke^{-kL}$. The matrix $\mathcal{M}_{ij}$ and the vector $\hat{\alpha}_i$ are obtained by performing a global fit to the experimental data. We use the fit of Ref. [15], which takes into account low-energy measurements, as well as the results from the Large Electron-Positron Collider runs 1 and 2 (LEP1 and LEP2), and the Stanford Linear Accelerator Center Large Detector (SLD). However, we have not included the NuTeV results.

Although the model contains a large number of parameters, some of these, or certain combinations of them, are fixed by the low-energy gauge couplings, fermion masses, and fermion mixing angles. Also, in order to avoid dangerous flavor-changing neutral currents we have considered family independent localization parameters, $c^{\text{light}}_{\xi_1}$, $c^{\text{light}}_{\xi_2}$, $c^{\text{light}}_{\xi_3}$, for the multiplets giving rise to the light SM fermions. A scan over parameter space shows that the EW fit favors the light RH quarks and leptons to be localized near the UV brane ($c^{\text{light}}_{\xi_2} \sim c^{\text{light}}_{\xi_3} \sim -0.6$) and the LH quarks and leptons to be localized close to each other. Thus, we will take a common localization parameter for the light LH quarks and leptons, denoted by c_{light}, and, unless otherwise specified, we place the light RH fermions near the UV brane (we denote their localization parameters by c_{RH}). Although the assumption of family independence is quite important when the fermions are localized near the IR brane, it is not essential when the fermions are localized closer to the UV brane (the fermion mass hierarchies can then be generated by exponential wave-function factors). In particular, if the light fermions are localized close to the UV brane, the results of our global fit apply even if their localization parameters are not family universal. As for the third quark family, we have allowed independent localization parameters for the different multiplets: c_1 for the multiplet giving rise to the $SU(2)_L$ doublet $(t, b)_L$, c_2 for the multiplet giving rise to t_R, and c_3 for the multiplet giving rise to b_R.

Regarding the localized mass mixing terms of Eq. (6), when the first two generations are localized near the IR brane, the corresponding terms are extremely small (of order $m_f/\tilde{k}$, where m_f is a fermion mass) and have a negligible effect. In this case, the only large boundary mass is M^{33}_u, which is fixed by the top-quark mass for each value of c_1 and c_2. However, when the light fermions are localized near the UV brane, the mixing mass terms can be of order 1 (recall these are dimensionless parameters). In this case, they can have an important effect on the KK spectrum. Nevertheless, they still have a negligible effect on the EW fit, for the following reasons. As discussed before, there are potentially important contributions from fermion KK modes both at tree and loop levels. The tree-level effects arise from mixing, after electroweak symmetry breaking, between the zero mode and the massive fermion modes, and can affect the couplings to the gauge bosons of the SM fermions. Since the region where the localized masses are of order 1 corresponds to the case where the zero-mode fermions are far from the IR brane, and since the mixing effects are proportional to the overlap between this wave function and the Higgs profile, which is localized near the IR brane, it is easy to see that the relevant mixing angles are exponentially suppressed. On the other hand, when the zero-mode fermions are near the IR brane, the localized masses are forced to be small due to the smallness of the light fermion masses, so that the mixing effects are again suppressed (for the down-type fermions, the custodial symmetry enforces additional cancellations). We have checked that these tree-level effects are always numerically negligible. The second class of potentially large effects arises at loop level. When the zero-mode fermions are near the IR brane, the loop effects are directly proportional to the fourth power of the small localized mixing parameters. When the zero-mode fermions are localized near the UV brane, although the loop contributions involving mixing with the zero mode are exponentially suppressed as above, there are loop contributions involving only mixing among massive KK states, which are not necessarily negligible. However, in this limit the massive KK spectrum is $SO(5)$ symmetric to a very good approximation. As a result, the loop contributions to the T parameter and the $Zb_L\bar{b}_L$ vertex discussed in the previous

section, due to the first two generations, are numerically negligible due to the custodial symmetry. We have also verified that the S parameter has only a weak dependence on the localized mixing masses. Thus, we conclude that, for the purpose of the EW fit analysis, the mixing masses involving the light generations can be neglected (although, of course, they are important in reproducing the correct fermion masses and mixing angles). Therefore, we are left with six relevant model parameters: $c_{\rm light}$, $c_{\rm RH}$, c_1, c_2, c_3, and $\tilde{k}$.

It should be noted that in models of gauge-Higgs unification the Higgs potential—that is induced at loop level—is also calculable [10]. Therefore, given the matter and gauge content of the model, the scale of new physics, $\tilde{k}$, is tied to the scale of EW symmetry breaking by the gauge and Yukawa couplings (the latter ones, as determined by the localized mass parameters). However, it is possible to imagine additional matter content that could affect the Higgs potential without having an impact on the EW precision measurements (e.g. 5D fermion multiplets without zero modes and with exotic quantum numbers that do not allow mixing with the SM fermions).[8] Therefore, we treat $\tilde{k}$ as an effectively independent parameter. Given the correlation between $\tilde{k}$ and the Higgs vev in any such model, one can use our bounds on $\tilde{k}$ to get an idea of whether the model is excluded or not (however, if $\tilde{k}$ turns out to be too small, an analysis that goes beyond the linear treatment of the Higgs couplings used here might be necessary). On the other hand, our approach allows us to apply our bounds to more general models with a bulk Higgs, and where the Yukawa couplings arise in a similar manner as in gauge-Higgs unification scenarios. We will also assume that, as happens in gauge-Higgs unification scenarios, the Higgs is light, and we have used a Higgs mass $m_H = 120$ GeV.

It was shown in Ref. [8] that the T parameter in models with custodial protection of the $Zb_L\bar{b}_L$ vertex is negative and non-negligible in a large region of parameter space. However, it exhibits a strong dependence on the right-handed top localization parameter, c_2, when the right-handed top has a nearly flat wave function, corresponding to $c_2 \sim -0.5$. In this case, T can easily reach positive values of order 1, so that by adjusting c_2 one can get essentially any value of T.[9] Thus, in order to reduce the dimension of our parameter space, we have chosen to minimize the χ^2 with respect to c_2 for each value of the rest of the parameters. Note that this also takes into account the loop corrections to the $Zb_L\bar{b}_L$ vertex, since these are correlated with the T parameter as exemplified in Fig. 1. By taking the RH fermions near the UV brane we are also minimizing with respect to $c_{\rm RH}$. We have therefore performed a four-parameter fit and obtained the 2σ bound on $\tilde{k}$ by varying the χ^2 with respect to the other three parameters, $c_{\rm light}$, c_1, and c_3. The first of these parameters, that determines the localization of the light fermions, affects directly the tree-level effective Lagrangian computed in Sec. III A, whereas the latter two, that involve localization of the third quark family, mostly enter the fit through the one-loop effects discussed in Sec. III B.

As we mentioned in Sec. II, the SM left-handed leptons can be embedded either in the vector or spinor representations of $SO(5)$. For the first choice, the left-handed SM leptons transform like $(\mathbf{2}, \mathbf{2})$ under the $SU(2)_L \times SU(2)_R$ subgroup, thus allowing for the implementation of the protection of some of the lepton couplings to the Z gauge boson, as done in the quark sector. Such a protection, however, is not as essential as in the quark sector, since all lepton masses are much smaller than the weak scale and they can be localized near the UV brane without inducing light KK states. This allows for the second possibility where the SM leptons transform like $(\mathbf{2}, \mathbf{1})$ or $(\mathbf{1}, \mathbf{2})$ under $SU(2)_L \times SU(2)_R$. As we show below, the bounds are somewhat relaxed for the second choice. Thus, we concentrate on this possibility, and mention the results of the fit when bidoublets are used for the leptons when appropriate.

A scan over parameter space gives a 2σ lower bound,

$$\tilde{k} \gtrsim 1 \text{ TeV} \quad (95\% \text{ C.L.}), \tag{17}$$

which in turn implies a mass for the first gauge KK excitations $m_1^{\rm gauge} \gtrsim 2.5$ TeV. This bound is saturated for $c_1 \approx 0.2$–0.3, $c_{\rm light} \approx 0.48$, and $c_3 \approx -0.55$ (with the RH light fermions localized near the UV brane and a nearly flat t_R wave function with $c_2 \approx -0.47$). On the other hand, when all the light fermions are localized near the UV brane, a bound of $\tilde{k} \gtrsim 1.4$ TeV is obtained, consistent with the result we found in Ref. [8] where a partial fit based on oblique parameters and the b asymmetries and branching fractions was used. This confirms the expectation that the partial fit captures the main effects of the new physics on the EW precision observables in the case that the light fermions are localized near the UV brane.

The results are actually quite insensitive to the value of c_1, with slightly better results as we get Q_1 farther from the IR brane, i.e. larger c_1. If Q_1 is too far from the IR brane, however, it is not possible to generate the top-quark mass, with a resulting upper bound $c_1 \lesssim 0.3$. In Fig. 2 we show, in the left panel, the 2σ lower bound on $\tilde{k}$ as a function of c_3 and $c_{\rm light}$, for fixed $c_1 = 0.2$, whereas in the right panel

[8]By adding additional matter multiplets without zero modes, but that break the $SU(2)_R$ symmetry by boundary conditions on the UV brane, it may be possible to induce additional contributions at one loop to observables such as the T parameter or the $Zb\bar{b}$ coupling. However, if one is restricted to models with a "minimal" matter content (with possible differences in the choice of boundary conditions and/or localized mass terms) we expect the qualitative features we found in our model to hold.

[9]We note here that in the case where the right-handed top arises from a triplet of $SU(2)_R$, as opposed to a singlet as studied in this work, there is also a narrow region around $c_2 \sim +0.5$, where the T parameter can be positive [8].

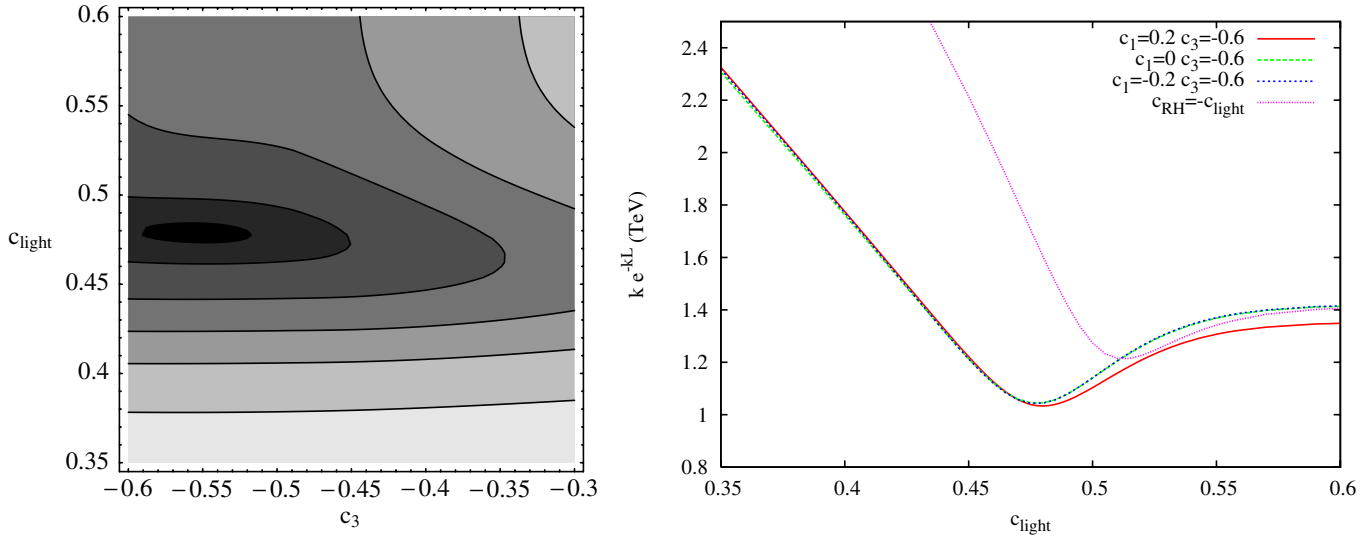

FIG. 2 (color online). Lower bound on $\tilde{k} = ke^{-kL}$ as a function of c_3 and c_{light} for fixed $c_1 = 0.2$ and $c_{\text{RH}} = -0.6$ (left panel). The different contours, from dark to light, correspond to $\tilde{k} = 1030$, 1100, 1300, 1500, 1700, and 2000 GeV, respectively. The minimum is $\tilde{k}_{\text{min}} = 1$ TeV, corresponding to $c_3 \approx -0.55$ and $c_{\text{light}} \approx 0.48$. In the right panel we show the lower bound on $\tilde{k}$ as a function of c_{light} for fixed $c_{\text{RH}} = c_3 = -0.6$ and three values of c_1. We also show the lower bound on $\tilde{k}$ for $c_1 = 0.2$ and $c_3 = -0.6$, assuming $c_{\text{RH}} = -c_{\text{light}}$. The mass of the first gauge KK modes is $m_1^{\text{gauge}} \approx 2.5\tilde{k}$.

we show the bound on $\tilde{k}$ as a function of c_{light} for fixed $c_3 = -0.6$ and three different values of $c_1 = -0.2$, 0, 0.2, displaying the mild dependence on this latter parameter. We also show in the same figure the effect of localizing the light RH quarks and leptons at the same point as the LH ones. The minimum of the fit then shifts to $-c_{\text{RH}} = c_{\text{light}} \approx 0.51$ with a lower bound $\tilde{k} \gtrsim 1.2$ TeV.

The dependence on the localization of the light fermions is easy to understand. The fit is virtually independent of the particular localization once the conformal point is crossed towards the UV brane, $c_{\text{light}} \gtrsim 0.5$, due to the universal couplings of fermion zero modes to gauge boson KK modes in that case. There is of course a limit on how far from the IR brane we can get, given by the fact that we have to generate the fermion masses. For instance, the charm and strange masses force us to take the associated localization parameters below about 0.6. This is why we have taken $c_{\text{light}} \leq 0.6$ in our plots. As we have emphasized, however, the results in that limit are independent of the particular localization of each light fermion, and we could take the first generation fermions to be farther away from the IR brane with similar results.

Also, as is clear from Fig. 2, bringing the light fermions very close to the IR brane does not improve the fit, due to the strong coupling to the gauge boson KK modes in that limit. However, the figure also shows a minimum when the light fermions are near the conformal point. It is well known that in this case the (light) fermions decouple from the KK excitations of the W and Z gauge bosons. It is nevertheless important to notice that they do not decouple from the KK excitations of the $SU(2)_R$ gauge bosons and, even near the conformal point, this leads to nonuniversal shifts in the gauge couplings of the SM fermions that cannot be neglected in the fit. To illustrate the relevance of such effects, if the custodial protection, $SU(2)_V \times P_{LR}$, is also implemented in the lepton sector, such nonuniversal shifts are enough to completely erase the dip in the χ^2 near the conformal point. In that case, one finds a 2σ lower bound of $\tilde{k} \gtrsim 1.4$ TeV, obtained when the light fermions are near the UV brane [this is exactly as in Fig. 2, since in this region the $SU(2)_R$ gauge bosons quickly decouple from the low-energy physics], and the bound increases monotonically as the light fermions are brought closer to the IR brane. Such a feature is a direct result of the fermion couplings to the $SU(2)_R$ gauge bosons as specified by the embedding into bidoublets of $SU(2)_L \times SU(2)_R$. We explore other possibilities in Sec. V.

Finally, the dependence on the last localization parameter, c_3, can also be easily understood. In the limit that the light fermions are near the IR brane ($c_{\text{light}} \leq 0.5$), the loss of up-down universality as well as the strong coupling of light fermions to the gauge boson KK excitations dominate the fit, and therefore the details of the b_R localization are irrelevant. This is the reason for the horizontal contours in the left panel of Fig. 2 for $c_{\text{light}} \lesssim 0.5$. As the light fermions get farther from the IR brane, the b asymmetries and branching fractions gain importance in the fit and therefore there is some dependence on the value of c_3. The fit shows that the EW precision observables select the region in which b_R and the RH light fermions are localized close to the UV brane, whereas the LH light fermions are near the conformal point slightly towards the IR brane. In such a

scheme the fermion mass hierarchies can be obtained from the RH fermion profiles. Note, however, that the light families, both LH and RH, could be localized close to the UV brane with only a slightly tighter bound on $\tilde{k}$.

V. EFFECTS OF SIMPLE MODIFICATIONS

The result of the global fit gives an excellent idea of the typical bounds on the scale of new physics in this class of models. Nevertheless, they are indirect bounds and they should be interpreted accordingly.

In particular, contrary to the T parameter and the $Zb_L\bar{b}_L$ coupling, which receive calculable corrections, the S parameter can get arbitrary corrections from physics at the ultraviolet cutoff, i.e. from a bulk operator that reduces to the operator of Eq. (12) after dimensional reduction.[10] If the size of the coefficient of such a bulk operator is estimated based on the rules of NDA [21,22], it is not difficult to see that these contributions are negligible compared to those arising from the physics below the cutoff. Nevertheless, such arguments do not exclude the existence of UV completions that would give a contribution to the S operator *larger* than the NDA estimate,[11] and therefore sizable contributions to the S parameter cannot be ruled out. In addition, as mentioned at the end of Sec. III B, we have not computed the one-loop contributions to S arising from gauge loops. To estimate the effect such contributions might have, we have repeated the global fit with a contribution to the S parameter that is twice as large as the one we have computed at one loop in our model. This gives us an idea of the effects that calculable contributions to S, such as those involving gauge bosons in the loop, might have. We have also redone the fit with an arbitrary contribution to the S parameter, which we have optimized for each value of the input parameters. This would correspond to the best case scenario where the UV physics induces an optimal S parameter, from the point of view of the fit, including in some cases a sizable and negative contribution to S. This exercise is useful to elucidate the role that the calculable contributions to the T parameter and to the $Zb\bar{b}$ coupling have in the EW fit. The results of such fits are shown in Fig. 3 with a solid line in the case of no extra contribution to the S parameter beyond the one we have computed, a dashed line for an extra contribution double the one we have computed in our model, and a dotted line in the case that the extra contribution to the S parameter has been optimized to minimize the χ^2. The figure shows that a moderate extra positive contribution to the S parameter worsens the fit slightly whereas optimizing the contribution leads to a considerably better fit, with a lower bound $\tilde{k} \gtrsim 650$ GeV (optimal S).[12] Of course, this latter possibility is the result of a model tuned to optimize the fit, most likely requiring a fine-tuned UV completion, and therefore should not be taken as generic. Also, for such low values of $\tilde{k}$ the approximations we have made in linearizing the couplings to the Higgs in the present gauge-Higgs unification scenarios may have to be revisited. Nevertheless, this exercise gives us an idea of how changes in the model (or, like in this case, effects of the UV completion of our model) can affect these bounds. In particular, a negative contribution to the S parameter can be interesting [24].

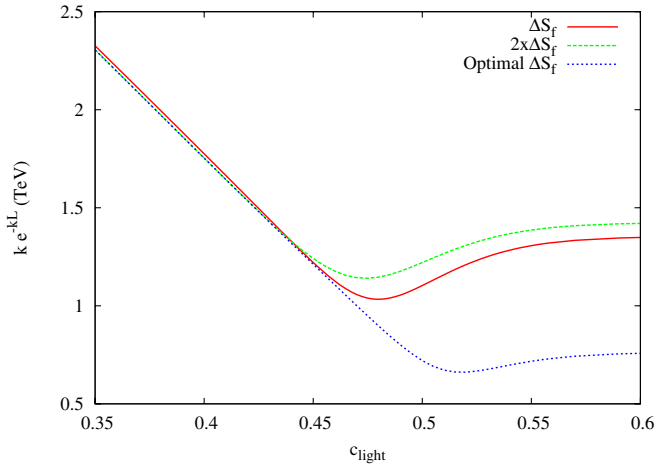

FIG. 3 (color online). Lower bound on $\tilde{k} = ke^{-kL}$ as a function of c_{light} allowing different contributions to the S parameter in the model of Sec. IV. The three lines correspond to the one-loop contribution from the spectrum in the model, Eq. (A26) (solid line), twice that amount (dashed line), and a value of ΔS_f that minimizes the χ^2 for each value of the parameters (dotted line). See discussion in the main text. In all cases, $c_1 = 0.2$ and $c_{\text{RH}} = c_3 = -0.6$.

A second type of modification is obtained when the quarks of the first two families—as in the lepton sector—arise from doublets of $SU(2)_L$ or $SU(2)_R$, as opposed to bidoublets of $SU(2)_L \times SU(2)_R$. In this case, it might be difficult to generate the mixing between the first two quark generations and the third one. Nevertheless, we have repeated the global fit analysis in such a scenario, as shown in Fig. 4. When the LH and RH fermions have a common localization parameter, $c_{\text{light}} = -c_{\text{RH}}$, the fit exhibits a

[10]The form of this bulk operator will be different in gauge-Higgs unification scenarios and in models with a fundamental Higgs field.

[11]We notice that this does not necessarily imply a complete loss of calculability resulting from strong coupling effects. For example, at one loop an insertion of the S operator can lead to contributions to the fermion vertex operators, Eqs. (9). Generically, such contributions would also be enhanced compared to the NDA estimate. However, it is possible that there are cancellations between the loop- and tree-level contributions so that the physics at the cutoff scale gives a small contribution to the fermion vertices, while giving a large contribution to S. Of course, such a situation would likely reflect a fine-tuned UV completion.

[12]In this case, the constraints arise from observables that depend on the b quark couplings, both at the Z peak and at LEP2 energies.

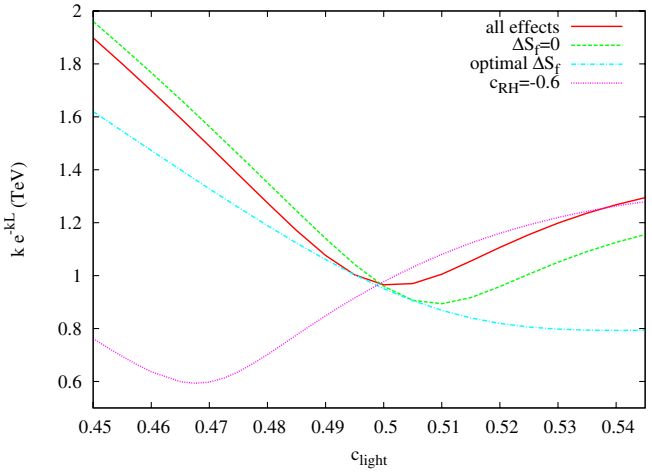

FIG. 4 (color online). Lower bound on $\tilde{k} = ke^{-kL}$ as a function of $c_{\text{light}} = -c_{\text{RH}}$ when the light generations arise from doublets of $SU(2)_L$ or $SU(2)_R$, including all effects (solid line), setting the one-loop contributions to ΔS_f to zero (dashed line), and choosing values of ΔS_f that minimize the χ^2 for each value of the parameters (dash-dotted line). We also show the lower bound on $\tilde{k}$ when the right-handed light fermions are localized at $c_{\text{RH}} = -0.6$ (near the UV brane), as a function of the localization parameter for left-handed light fermions, c_{light} (dotted line). In all cases we have fixed $c_1 = 0.2$ and $c_3 = -0.6$.

minimum corresponding to a 2σ bound of $\tilde{k} \approx 1$ TeV, again around $c_{\text{light}} \approx 0.5$. This corresponds to the conformal point, where the light generations decouple from the KK modes of the $SU(2)_L$ gauge bosons (solid line). Note, however, that this fit includes the fermion one-loop contributions to the S parameter, ΔS_f, that are sizable. If we do not include such loop contributions, the fit prefers that the light generations be localized somewhat closer to the UV brane (dashed line). This is contrary to the naive expectations, since when the presence of the $SU(2)_R$ gauge bosons is taken into account, the tree-level corrections to the couplings between the left-handed SM fermions and the gauge bosons vanish at a point slightly closer to the IR brane. The result we find can be explained by observing that, under the assumption $c_{\text{RH}} = -c_{\text{light}}$, we cannot simultaneously avoid the corrections to the couplings involving left- and right-handed fermions, and the global fit still prefers a region of parameter space where the couplings to the $SU(2)_R$ gauge bosons are somewhat suppressed (fermions closer to the UV brane). In fact, when the light RH quarks and leptons are localized near the UV brane, the fit shows a clear and pronounced minimum at $c_{\text{light}} \approx 0.47$. In that case, one finds a lower bound on $\tilde{k} \gtrsim 600$ GeV, due to an improvement in A_{FB}^b resulting from a decrease in A_e. Finally, we have redone the fit, again for $c_{\text{RH}} = -c_{\text{light}}$, with an arbitrary contribution to the S parameter, optimized to minimize the χ^2 (dash-dotted line). As previously discussed, such a scenario could arise from a (possibly fine-tuned) UV completion.

We therefore conclude that both the calculable loop corrections and various sources of nonuniversal shifts to the couplings between fermions and gauge bosons can place important restrictions, and that a global fit analysis is essential in a broad class of warped scenarios, whenever the light generations are not close to the UV brane. We find that the indirect bounds on $\tilde{k}$ are typically around a TeV.

VI. SPECTRUM AND PHENOMENOLOGICAL IMPLICATIONS

We have seen that a global fit to EW precision observables allows KK excitations of the SM gauge bosons, together with $W_R^{\pm}$ and Z', as light as $m_1^{\text{gauge}} \sim 2$–$3$ TeV over a wide region of parameter space in models with custodial protection of the T parameter and the $Zb_L\bar{b}_L$ coupling. This opens up exciting possibilities for discovering these particles at the LHC and measuring their properties [25]. In particular, the loop contribution to the T parameter typically singles out a very specific localization of the third quark family [t_R almost flat and (t_L, b_L) near the IR brane], which leads to a distinct phenomenology.[13] The fermionic spectrum is even more exciting, as it can be much lighter than the spectrum of gauge boson KK modes. There are two reasons why KK fermions can be light in these models. One is the presence of large brane localized masses, and the other is the natural appearance of twisted boundary conditions, $(-, +)$ or $(+, -)$. Large brane localized masses, needed to generate the large top mass, are a generic feature of these models. In principle, one could get the top mass through brane localized masses that connect either bidoublets or singlets [see Eq. (6)]. However, in the case of localized masses connecting two bidoublets, the light KK bidoublet excitations will mix strongly with the top quark, inducing a negative T parameter which is disfavored by the EW precision data. Thus, the top mass should be predominantly obtained by means of brane localized masses connecting singlets, and therefore light KK singlets are a generic prediction in these theories. On the other hand, light KK fermion bidoublets can arise from twisted boundary conditions, provided they do not mix strongly with the zero modes. In particular, our boundary conditions for Q_2, which ensure no mixing between the bidoublets Q_1 and Q_2, give quarks much lighter than $\tilde{k}$ provided that the t_R wave function is nearly flat (i.e. $c_2 \sim -0.5$), as required by the EW precision data.

The typical fermionic spectrum in our model is shown in Tables I and II. For each of the first two families, the four quarks in Q_2 of Eq. (5) have very light KK excitations for $c_{\text{RH}} \lesssim -0.5$ [18,26]. As shown in Table I, there are eight quarks with almost degenerate masses of a few hundred GeV. Four of them have charge $2/3$, and

[13]This interesting possibility, mentioned for the first time in [8], with the (t_L, b_L) quarks coupling more strongly to the IR brane than t_R, was briefly discussed in [25].

TABLE I. Electric charges, typical masses, and decay channels for the KK excitations of the first two quark families with masses below 1 TeV. Here, q_1^i and q_2^i are linear combinations of the gauge eigenstates q'^{u_i} and $\chi_2^{d_i}$ of Eq. (5).

q'	Q	$m_{q'}$ (GeV)	Decay
q_1^1	$\frac{2}{3}$	~200–500	$q_1^1 \to Zu$ (100%)
q_1^2	$\frac{2}{3}$	~200–500	$q_1^2 \to Zc$ (100%)
q_2^1	$\frac{2}{3}$	~200–500	$q_2^1 \to Hu$ (100%)
q_2^2	$\frac{2}{3}$	~200–500	$q_2^2 \to Hc$ (100%)
$\chi_2^{u_1}$	$\frac{5}{3}$	~200–500	$\chi_2^{u_1} \to Wu$ (100%)
$\chi_2^{u_2}$	$\frac{5}{3}$	~200–500	$\chi_2^{u_2} \to Wc$ (100%)
q'^{d_1}	$-\frac{1}{3}$	~200–500	$q'^{d_1} \to Wu$ (100%)
q'^{d_2}	$-\frac{1}{3}$	~200–500	$q'^{d_2} \to Wc$ (100%)

two decay almost exclusively to $Z + j$ (where j denotes a jet from an up or charm quark) while the other two decay to $H + j$. There are also two light quarks with charge $-1/3$ and two with exotic charge $5/3$, which decay to $W + j$.

For the third family, we have three essentially degenerate KK excitations with charges $5/3$, $2/3$, and $-1/3$. There is a fourth KK excitation with charge $+2/3$ and a mass very close to the previous states. In Fig. 5 (left panel), we show the variation of the masses of the three lightest, degenerate KK quark excitations—that couple strongly to the third generation—as functions of the basic parameters of the model, for fixed $c_1 = 0.2$ and $\tilde{k}$ saturating the lower bound from the global fit that assumes a common localization parameter for all the light fermions (both LH and RH chiralities). Figure 5 (right panel) shows the masses of the three lightest KK modes with charge $2/3$ as a function of c_{light} for fixed values of $c_1 = 0.2$ and $c_3 = -0.6$. As seen in the figures, quarks as light as about 400 GeV are allowed in the region in which the light fermions are near the conformal point and b_R is near the UV brane.

TABLE II. Electric charges and typical masses and decay channels for the KK excitations of the third quark family with masses below 1 TeV. We have fixed $c_{\text{light}} = -c_{\text{RH}} = 0.52$, $c_1 = 0.2$, $c_2 = -0.49$, $c_3 = -0.6$, and $\tilde{k} = 1.2$ TeV. Here, q_1, q_2, and u_2 are mainly admixtures of the gauge eigenstates q'^{u_3}, $\chi_2^{d_3}$, and u'^3 of Eq. (5).

q'	Q	$m_{q'}$ (GeV)	Decay
q_1	$\frac{2}{3}$	369	$q_1 \to Zt$ (20%) $q_1 \to Ht$ (60%) $q_1 \to Wb$ (20%)
q_2	$\frac{2}{3}$	373	$q_2 \to Zt$ (9%) $q_2 \to Ht$ (70%) $q_2 \to Wb$ (21%)
u_2	$\frac{2}{3}$	504	$u_2 \to Zt$ (13%) $u_2 \to Ht$ (40%) $u_2 \to Wb$ (41%) $u_2 \to Zq_1$ (1.5%) $u_2 \to Wq'^{d_3}$ (2.5%) $u_2 \to W\chi_2^{u_3}$ (2.%)
$\chi_2^{u_3}$	$\frac{5}{3}$	369	$\chi_2^{u_3} \to Wt$ (100%)
q'^{d_3}	$-\frac{1}{3}$	369	$q_2'^{d_3} \to Wt$ (100%)

As an example, we show in Table II the typical values for the light KK excitations for the third family when $c_{\text{light}} = -c_{\text{RH}} = 0.52$, $c_1 = 0.2$, $c_2 = -0.49$, $c_3 = -0.6$, $\tilde{k} = 1.2$ TeV, and localized mass parameters such that the SM quark masses and CKM matrix are correctly reproduced. There are three quarks with charge $2/3$, two of them with almost degenerate masses of about 370 GeV and the third one with mass of about 500 GeV. All of them have decays to $Z + t$, $H + t$, and $W + b$, as shown in the table. There are also two other light KK modes, one with charge $-1/3$ and another with exotic charge $5/3$, with degenerate masses of order 370 GeV and which decay almost exclusively to $W + t$. Note that there is a small but non-negligible probability for the heavier of the three quarks with charge $2/3$ to decay into the quarks of mass ~370 GeV (with either charge).

The rest of the fermion KK modes have masses typically above 1 TeV. In the following we shall discuss the potential for searches for the first level of fermionic excitations at the Tevatron and the LHC. These models can also have very interesting collider implications in bottom and top physics [27,28] but we postpone their study for future work.

A. Fermion KK modes at the Tevatron

The Tevatron has excellent capabilities to search for the light KK excitations of the first two generation quarks shown in Table I. In particular, there are ongoing Tevatron searches for heavy quarks decaying to $W + j$ [29] and $Z + j$ [30], which apply directly to our model. The first analysis examines the $W + j$ mass spectrum and compares to the distribution expected from a generic fourth-generation top quark. The $Z + j$ analysis does not assume any specific model, but rather looks at the tail of the jet energy distribution for an excess above the SM expectation. A similar analysis looks at the p_T distribution of the Z boson, and in principle could also be sensitive to signals from our model. Using the results of these analyses and taking into account the enhancement factor in the production cross section due to the multiplicity of quarks (4 in the $W + j$ analysis and 2 in the $Z + j$ one), we obtain the following lower bound on the mass of the light KK excitations:

$$m_q \geq \begin{cases} 325\,(410)\,\text{GeV}, & W + j \text{ with } 0.76\,(\text{projected } 8)\,\text{fb}^{-1}, \\ 300\,\text{GeV}, & Z + j. \end{cases} \tag{18}$$

Figure 6 shows the bound on $\tilde{k}$ from the fit to EW precision

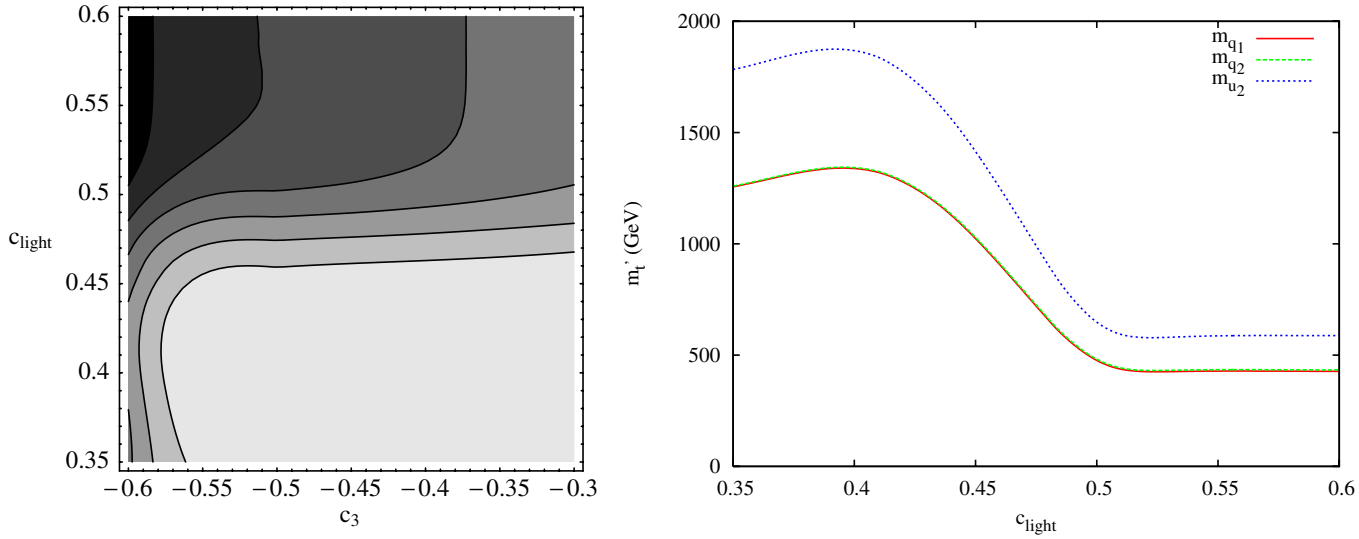

FIG. 5 (color online). Mass of the first level quarks of the third generation for the model of Sec. IV and a $\tilde{k}$ that saturates the bound, assuming $c_{\mathrm{RH}} = -c_{\mathrm{light}}$ (dotted curve in the right panel of Fig. 2). In the left panel we show the masses of the three degenerate quarks with charges $5/3$, $2/3$, and $-1/3$ as a function of c_3 and c_{light}, for fixed $c_1 = 0.2$. The different contours, from dark to light, correspond to $m_1 = 500$, 600, 750, 1000, 1250, and 1500 GeV, respectively. In the right panel we show the mass of the three lightest quark KK modes with charge $2/3$ as a function of c_{light} for fixed $c_1 = 0.2$ and $c_3 = -0.6$.

data together with the constraints on our parameter space that result from these direct searches at the Tevatron. The direct search analysis eliminates the region of parameter space in which the light fermions are localized towards the UV brane.[14] When combined with the EW precision analysis, they slightly strengthen the lower bound on $\tilde{k}$.

Final states with Z bosons could also lead to a signature with missing energy and jets. Searches for squarks and gluinos might be sensitive to a signal of this type. It is difficult to relate the experimental results to our model without performing detailed simulations. However, this channel might become interesting with a sufficiently large integrated luminosity.

We have considered other searches at the Tevatron, such as the trilepton, same-sign di-lepton, and four-lepton searches. However, these are usually rather model dependent and apply cuts which tend to eliminate our signal. In particular, leptons reconstructing the Z mass peak as well as jets are typically disallowed.

A very interesting feature is the presence of two light quarks that decay exclusively into $H + j$. If these quarks have masses around 300 GeV, their production cross section will be of the same order of magnitude as Higgs production through gluon fusion for a light Higgs. As there are two such quarks, and two Higgs bosons in every event, there will be a sizable enhancement to the inclusive Higgs signal. It should be noted, however, that some sources of background (such as WW + jets or ZZ + jets) are also enhanced due to the decays of other light KK excitations, and a careful analysis of signal and background is necessary to assess Tevatron prospects for Higgs discovery in this model.

Finally, the KK excitations of the third quark generation, as shown in Table II, are on the verge of the projected sensitivity for the Tevatron.

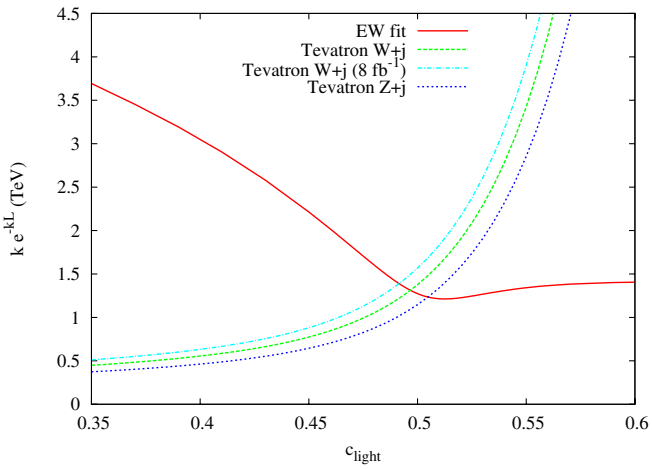

FIG. 6 (color online). Lower bound on $\tilde{k} = ke^{-kL}$ as a function of $c_{\mathrm{light}} = -c_{\mathrm{RH}}$ for fixed $c_1 = 0.2$ and $c_3 = -0.6$. The different lines correspond to the bounds from EW precision observables (solid line), the W + jets analysis at Tevatron with 0.76 fb^{-1} (dashed line), the projected exclusion reach to 8 fb^{-1} in that same channel (dotted-dashed line), and Z + jets analysis at Tevatron (dotted line). The regions below the curves are excluded.

[14]But notice that these direct bounds can be evaded by switching the boundary conditions for Q_2 in Eq. (5) for the first two generations.

B. Fermion KK modes at the LHC

The prospects for discovery of the light KK quark excitations of the first two families are more promising at the LHC. In principle, similar techniques as those used at the Tevatron could lead directly to a discovery, although the increase in production comes at the cost of a larger background from di-boson and top-quark production.

Quarks decaying to $H + j$ enhance Higgs production at the LHC with respect to the standard model. This cross section is of the same order as Higgs gluon fusion production, provided the quarks are not much heavier than about 400 GeV. If the Higgs is heavy enough to decay to ZZ we have the following enhanced contribution to the inclusive $H \to ZZ$ cross section,

$$\sigma(H \to ZZ)_{\text{incl}} \approx 2\sigma(q'\bar{q}')B[2 - B] + \sigma(gg \to H)B, \tag{19}$$

where we have included the multiplicity of the KK fermions, and where $B \equiv \text{BR}(H \to ZZ) \sim 0.02$–$0.25$ for $m_H \sim 120$–200 GeV [31]. For these values of B, there can easily be an enhancement in the inclusive $H \to ZZ$ of order a few. Note that there is also a contribution to the background from quarks decaying to $Z + j$, although the mass reconstruction in this channel seems precise enough to efficiently cut that background. Another clean channel would be $H \to \gamma\gamma$ for which we can take advantage of the enhancement of Higgs production without suffering a larger background from the decays of the lighter KK modes. Note that the contribution of the extra quark states to the loop-induced couplings, such as $gg \to H$ and $H \to \gamma\gamma$, is small. The reason is that these heavy quark states receive only a very small contribution to their masses from EW symmetry breaking, and as a result their effective (diagonal) Yukawa couplings are very suppressed. However, these states can mix strongly with the top quark, resulting in a smaller top Yukawa coupling that can significantly reduce the Hgg vertex.

There is an important distinction to be made between the first two generations and the third one. While the Tevatron is able to probe masses on the order of 300 GeV or higher, these constraints can be evaded for the first two generations. If we switch the boundary conditions of the multiplet Q_2 for the first two families, the excitations of the first two quark generations become heavier, without affecting the EW fit. In that case the zero modes for the first two generations can be localized near the UV brane and the nice features of the mass generation through wave function suppressions preserved, as well as the flavor universality of the corrections (which become independent of the particular localization parameter in this limit). Nonetheless, the KK quark excitations of the third quark generation remain light, and well within the reach of the LHC [32,33] (and possibly of the Tevatron).

Also for the third generation, the degenerate doublets with different hypercharges and large mixings with singlets give additional Higgs production channels which will greatly enhance the signals in inclusive Higgs searches and searches in the ttH channel. The Higgs discovery reach will be even better than the one found in previous studies [34], which considered singlets, due to the enhanced decay ratio to Higgs (~ 40–70% vs 25% for singlets).

One will notice that nearly all of the final states listed in Table II result in top quarks in the final state. This suggests that inclusive top searches would be useful for finding these particles at the LHC. Another interesting signature might be multiple jets, some of them with b quarks, and possibly high-p_T leptons or missing energy.

Finally, the exotic quantum numbers of the fermion KK excitations of the third generation can give rise to spectacular new signatures. For instance, the quarks with electric charges $5/3$ and $-1/3$ have similar decay channels with four W's,

$$q'\bar{q}' \to W^+W^-t\bar{t} \to W^+W^+W^-W^-b\bar{b}. \tag{20}$$

This can lead to a very clean final state $e^+e^+\mu^-\mu^- + b\bar{b} + \not{E}_T$ with very little background. Furthermore, for the charge $5/3$, we have two W's of the same charge belonging to the same decay chain, which could be identified by a pair of same-sign leptons. Also, as seen in Table II, u_2 has a non-negligible branching fraction into the lighter charge $2/3$ states, which can lead to a spectacular signal with a $6Wb\bar{b}$ final state.

VII. CONCLUSIONS

Models with warped extra dimensions explain in a compelling way the hierarchy between the Planck and EW scales. Bulk fermions provide also a rationale for the observed hierarchy of fermion masses and the absence, for the light fermions, of large flavor changing neutral currents or large new effects from physics above the ultraviolet cutoff of the theory. The SM gauge bosons and third generation quarks, however, have a sizable coupling to heavy states through the Higgs field. These couplings induce large corrections to the T parameter and the coupling of the left-handed bottom quark to the Z gauge boson unless some symmetry forbids them. An enlarged bulk gauge symmetry can act as a custodial symmetry, $SU(2)_V \times P_{LR}$, that protects both the T parameter and the $Zb_L\bar{b}_L$ coupling. When such a symmetry is broken only on the UV brane, these two observables acquire a distinctive status: they are insensitive to UV physics except for effects that are suppressed by a scale of order M_{Pl}. This means that, for all practical purposes, they are calculable. We find that, typically, the one-loop corrections to these observables are sufficiently important that they need to be included when analyzing the bounds on these models. Furthermore, for the fermion quantum numbers required to obtain the SM fermions while preserving the custodial symmetry, these loop corrections are correlated. Thus, they are a generic feature of models with warped extra dimen-

sions and custodial symmetry $SU(2)_V \times P_{LR}$, no matter whether the Higgs is a fundamental scalar, the extra dimensional component of a gauge field (gauge-Higgs unification), or not present (Higgsless models). The precise values of the T parameter and the $Zb_L\bar{b}_L$ coupling are model dependent, but we have identified the contributions that are generically present under the assumption of a custodial symmetry.

We have illustrated these features in a particular model of gauge-Higgs unification. We have computed all the relevant tree-level effects on EW precision observables plus the leading one-loop corrections to the T parameter and the $Zb_L\bar{b}_L$ coupling. By performing a global fit to all relevant EW precision observables, we have obtained a lower bound on the masses of the gauge boson KK excitations of about 2.5 TeV. This bound is saturated when the left-handed light fermions have nearly flat wave functions (the conformal point), while the right-handed light fermions are localized near the UV brane. However, very similar bounds are found in a large region of parameter space in which all the light fermions are localized far from the IR brane. In the latter case, the fit is dominated by a universal shift of the fermion coupling to the SM gauge bosons that can be redefined into a pure oblique correction to the S parameter, although the correlation between the T parameter and the $Zb_L\bar{b}_L$ coupling also has a noticeable effect. Contrary to these two latter observables, the S parameter is not protected by any symmetry and can receive corrections from physics above the UV cutoff. Assuming an optimal correction to the S parameter from UV physics, such that the χ^2 of the fit is minimized with respect to S for each point in parameter space, we have obtained a lower bound on the mass of the gauge boson KK modes of $\sim$1.6 TeV, which is completely dominated by the observables in the b sector and is therefore difficult to evade (as those observables are dominated by the $Zb_L\bar{b}_L$ coupling that is calculable in these models).

Regarding the fermionic spectrum, there can be a wealth of new vectorlike quarks with exotic quantum numbers and masses as low as a few hundred GeV. These modes can be light enough for the Tevatron to have started probing part of the parameter space. We have discussed the bounds that current Tevatron analyses place on our model. Interestingly enough, some of these modes have exotic decay channels, for instance, some of them decaying essentially 100% into H plus jets. This opens up interesting prospects for Higgs physics both at the Tevatron and the LHC. Heavy quarks decaying to $W + j$ or $Z + j$ have been searched for at the Tevatron, with current limits of about 325 GeV and 300 GeV, respectively, for the quark multiplicities present in our model. Excitations of the third generation quarks can have masses of order 400 GeV that might be within reach of the Tevatron. They typically decay to third generation quarks with nonstandard branching ratios, naturally enhancing Higgs production. Decays to top quarks through gauge bosons induce a very interesting decay chain with four gauge bosons ($4W$ or $2W + 2Z$) and two b's, as well as a possible final state with six W's and two b's that would give a spectacular signal at the LHC. In particular, heavy quarks (with typical masses of order 500 GeV) with electric charge $5/3$ produce two same-sign W in each decay chain, whereas those with charge $-1/3$ will give one W of each sign per chain. The process

$$\begin{aligned} pp &\to q_{5/3,-1/3}\bar{q}_{5/3,-1/3} \to W^+tW^-\bar{t} \\ &\to W^+W^+bW^-W^-\bar{b} \to \mu^+\mu^+e^-e^-b\bar{b}\not{E}_T \end{aligned} \tag{21}$$

would lead to an easy discovery of these modes with almost no background.

ACKNOWLEDGMENTS

We would like to thank Z. Han and W. Skiba for useful comments on the fits in [15]. We would also like to thank A. Attal, R. Erbacher, S. Nikitenko, and A. Scott for providing helpful experimental input, and, in particular, J. Conway and M. Schmitt for many useful discussions. C. E. M. Wagner thanks N. Shah and A. Medina for useful comments. Work at ANL is supported in part by the U.S. DOE, Div. of HEP, Contract No. DE-AC-02-06CH11357. Fermilab is operated by Fermi Research Alliance, LLC under Contract No. DE-AC02-07CH11359 with the U.S. DOE. E. P. was supported by the DOE under Grant No. DE-FG02-92ER-40699.

Note added.—During the final stages of this article, we received Refs. [35,36], which partially overlap with ours in the study of different aspects of models with warped extra dimensions and custodial protection of the $Zb_L\bar{b}_L$ coupling. However, they do not discuss the importance of the calculable one-loop corrections to the T parameter or the $Zb_L\bar{b}_L$ coupling, nor perform a detailed global fit to the EW precision observables.

APPENDIX: 4D EFFECTIVE THEORY

In this appendix we give the details of the matching between the 5D theory and the 4D theory used to perform the global fit analysis. We compute the dimension-six operators and put them in the form of Eq. (7).

1. Integration of heavy gauge bosons

We can perform the tree-level integration of heavy gauge bosons in an $SU(2)_L \times U(1)_Y$ gauge invariant way by splitting the full covariant derivative into a *standard model* part and a part involving heavy physics,

$$\begin{aligned} D_\mu^{\text{full}} = D_\mu - i[&g_{5L}\tilde{W}^a_{L\mu}T^a_L + g_{5R}\tilde{W}^b_{R\mu}T^b_R + g'_5 Y\tilde{B}_\mu \\ &+ g_{5Z'}Q_{Z'}\tilde{Z}'_\mu], \end{aligned} \tag{A1}$$

where D_μ represents the SM covariant derivative and we use tildes to denote the massive KK components of the 5D fields. In the above, $a = 1, 2, 3$ label the $SU(2)_L$ gauge

bosons, $b = 1, 2$ label the charged $SU(2)_R$ gauge bosons, and B_μ and Z'_μ are the following two combinations of neutral gauge bosons,

$$B_\mu = \frac{g_{5X} W^3_{R\mu} + g_{5R} X_\mu}{\sqrt{g^2_{5R} + g^2_{5X}}}, \qquad Z'_\mu = \frac{g_{5R} W^3_{R\mu} - g_{5X} X_\mu}{\sqrt{g^2_{5R} + g^2_{5X}}}, \tag{A2}$$

with g_{5R}, g_{5X} the five-dimensional coupling constants of the $SU(2)_R$ and $U(1)_X$ groups,[15] respectively, while the hypercharge and Z' gauge couplings are

$$g'_5 = \frac{g_{5R} g_{5X}}{\sqrt{g^2_{5R} + g^2_{5X}}}, \qquad g_{5Z'} = \sqrt{g^2_{5R} + g^2_{5X}}. \tag{A3}$$

The charges are

$$\frac{Y}{2} = T^3_R + Q_X, \qquad Q_{Z'} = \frac{g^2_{5R} T^3_R - g^2_{5X} Q_X}{g^2_{5R} + g^2_{5X}}, \tag{A4}$$

so that the electric charge is

$$Q = T^3_L + T^3_R + Q_X. \tag{A5}$$

The Lagrangian involving heavy fields then reads (terms with two heavy fields except for kinetic terms give higher-order corrections and are therefore not written)

$$\begin{aligned}\Delta\mathcal{L} = {} & \tfrac{1}{2}\tilde{W}^a_{L\mu}\mathcal{O}^{\mu\nu}\tilde{W}^a_{L\nu} + \tfrac{1}{2}\tilde{W}^b_{R\mu}\mathcal{O}^{\mu\nu}\tilde{W}^b_{R\nu} + \tfrac{1}{2}\tilde{B}_\mu\mathcal{O}^{\mu\nu}\tilde{B}_\nu \\ & + \tfrac{1}{2}\tilde{Z}'_\mu\mathcal{O}^{\mu\nu}\tilde{Z}'_\nu + g_{5L}\tilde{J}^{a\mu}_L\tilde{W}^a_{L\mu} + g_{5R}\tilde{J}^{b\mu}_R\tilde{W}^b_{R\mu} \\ & + g'_5\tilde{J}^\mu_Y\tilde{B}_\mu + g_{5Z'}\tilde{J}^\mu_{Z'}\tilde{Z}'_\mu,\end{aligned} \tag{A6}$$

where

$$\mathcal{O}^{\mu\nu} \equiv [\eta^{\mu\nu}\partial^2 - \partial^\mu\partial^\nu + \eta^{\mu\nu}\partial_y(e^{-2ky}\partial_y)], \tag{A7}$$

and the effective currents read

$$\tilde{J}^{a\mu}_L = e^{-2\sigma}[(T^a_L h)^\dagger \mathrm{i}D^\mu h + \mathrm{H.c.}] + e^{-3\sigma}\bar{\psi}\gamma^\mu T^a_L\psi, \tag{A8}$$

$$\tilde{J}^{b\mu}_R = e^{-2\sigma}[(T^b_R h)^\dagger \mathrm{i}D^\mu h + \mathrm{H.c.}] + e^{-3\sigma}\bar{\psi}\gamma^\mu T^b_R\psi, \tag{A9}$$

$$\tilde{J}^\mu_Y = e^{-2\sigma}[(Yh)^\dagger \mathrm{i}D^\mu h + \mathrm{H.c.}] + e^{-3\sigma}\bar{\psi}\gamma^\mu Y\psi, \tag{A10}$$

$$\tilde{J}^\mu_{Z'} = e^{-2\sigma}[(Q_{Z'} h)^\dagger \mathrm{i}D^\mu h + \mathrm{H.c.}] + e^{-3\sigma}\bar{\psi}\gamma^\mu Q_{Z'}\psi. \tag{A11}$$

The equations of motion for the heavy fields can now be easily written and solved. For instance, for $\tilde{W}^a_L$, the equations of motion are

$$\mathcal{O}^{\mu\nu}\tilde{W}^a_{L\nu} = -g_{5L}\tilde{J}^{a\mu}_L, \tag{A12}$$

with the solution

$$\tilde{W}^a_{L\mu}(p; y) = g_{5L}\int_0^L \mathrm{d}y' \tilde{G}^{(++)}_{\mu\nu}(p; y, y')\tilde{J}^{a\nu}_L(p; y'), \tag{A13}$$

where $\tilde{G}^{(++)}_{\mu\nu}$ is the propagator for the KK modes obeying $(+, +)$ boundary conditions (the inverse of the differential operator in Eq. (A12) with the zero mode subtracted), and p is the four-dimensional momentum. Inserting the solution for all the heavy modes back into the Lagrangian, we obtain the following dimension-six effective Lagrangian:

$$\begin{aligned}\Delta\mathcal{L}_6 = \frac{1}{2}\int_0^L \mathrm{d}y\mathrm{d}y' [& g^2_{5_L}\tilde{J}^{a\mu}_L\tilde{G}^{(++)}_{\mu\nu}\tilde{J}^{a\nu}_L + g'^2_5\tilde{J}^\mu_Y\tilde{G}^{(++)}_{\mu\nu}\tilde{J}^\nu_Y \\ & + g^2_{5_R}\tilde{J}^{b\mu}_R\tilde{G}^{(-+)}_{\mu\nu}\tilde{J}^{b\nu}_R + g^2_{5Z'}\tilde{J}^\mu_{Z'}\tilde{G}^{(-+)}_{\mu\nu}\tilde{J}^\nu_{Z'}].\end{aligned} \tag{A14}$$

Note that these are already operators of dimension six. Thus, the propagators have to be evaluated at zero momentum. The relevant expression is

$$\tilde{G}_{\mu\nu}(p = 0, y, y') = \eta_{\mu\nu}\tilde{G}_{p=0}(y, y') + \mathcal{O}(p^2), \tag{A15}$$

where for $(+, +)$ boundary conditions,

$$\begin{aligned}\tilde{G}^{(++)}_{p=0}(y, y') = \frac{1}{4k(kL)}\Big\{ & \frac{1 - e^{2kL}}{kL} + e^{2ky_<}(1 - 2ky_<) \\ & + e^{2ky_>}[1 + 2k(L - y_>)]\Big\},\end{aligned} \tag{A16}$$

while for $(-, +)$ boundary conditions,

$$\tilde{G}^{(-+)}_{p=0}(y, y') = -\frac{1}{2k}[e^{2ky_<} - 1]. \tag{A17}$$

Here $y_<$ ($y_>$) denote the smallest (largest) of y and y', the fifth-dimensional coordinate.

The full y dependence of the effective Lagrangian can be encoded in the following coefficients,

$$\delta^2_{++} = \frac{L}{2}\int_0^L \mathrm{d}y\mathrm{d}y' e^{-2ky} f^2_H(y)\tilde{G}^{(++)}_0(y, y')e^{-2ky'} f^2_H(y'), \tag{A18}$$

$$G^{++}_\psi = \frac{1}{2}\int_0^L \mathrm{d}y\mathrm{d}y' |f_\psi(y)|^2\tilde{G}^{(++)}_0(y, y')e^{-2ky'} f^2_H(y'), \tag{A19}$$

$$G^{++}_{\psi\tilde{\psi}} = \frac{1}{L}\int_0^L \mathrm{d}y\mathrm{d}y' |f_\psi(y)|^2\tilde{G}^{(++)}_0(y, y')|f_{\tilde{\psi}}(y')|^2, \tag{A20}$$

with similar definitions for δ^2_{-+}, G^{-+}_ψ, and $G^{-+}_{\psi\tilde{\psi}}$ in terms of the propagator of Eq. (A17). We have used the y dependence of the fermion and Higgs zero modes,

$$\psi(x, y) = \frac{e^{3\sigma/2}}{\sqrt{L}} f_\psi(y)\psi(x) + \ldots, \tag{A21}$$

[15] In models that incorporate the P_{LR} symmetry, including the gauge-Higgs unification model based on $SO(5) \times U(1)_X$ studied in the main text, one has $g_{5R} = g_{5L}$.

$$h(x, y) = f_H(y)h(x) + \ldots, \tag{A22}$$

with the Higgs field $h(x)$ written here as a doublet of $SU(2)_L$. Technically, the fermionic dependence is more complicated due to the nontrivial mass mixing on the brane. The analysis of Ref. [15], however, assumes flavor universality for the first two families, and that will actually be a very good approximation for the range of parameters we will consider in the global fit (otherwise, large flavor violation involving the first two families would be generated, in gross conflict with experimental data).

Note that, even after evaluation of the propagators at zero momentum and integration over the extra dimension, the effective Lagrangian in Eq. (A14) is not yet in the basis of [14]. Simple manipulations of the operators involving integration by parts and use of the completeness of the Pauli matrices takes us to the desired basis. The resulting effective Lagrangian then reads

$$\begin{aligned}\Delta\mathcal{L}_6 = {} & \alpha_h\mathcal{O}_h + \alpha^t_{hl}\mathcal{O}^t_{hl} + \alpha^t_{hq}\mathcal{O}^t_{hq} + \alpha^s_{hl}\mathcal{O}^s_{hl} + \alpha^s_{hq}\mathcal{O}^s_{hq} \\ & + \alpha_{hu}\mathcal{O}_{hu} + \alpha_{hd}\mathcal{O}_{hd} + \alpha_{he}\mathcal{O}_{he} + \alpha^t_{ll}\mathcal{O}^t_{ll} \\ & + \alpha^t_{lq}\mathcal{O}^t_{lq} + \alpha^s_{ll}\mathcal{O}^s_{ll} + \alpha^s_{lq}\mathcal{O}^s_{lq} + \alpha_{le}\mathcal{O}_{le} + \alpha_{qe}\mathcal{O}_{qe} \\ & + \alpha_{lu}\mathcal{O}_{lu} + \alpha_{ld}\mathcal{O}_{ld} + \alpha_{ee}\mathcal{O}_{ee} + \alpha_{eu}\mathcal{O}_{eu} \\ & + \alpha_{ed}\mathcal{O}_{ed} + \ldots,\end{aligned} \tag{A23}$$

where the list of operators was given in Eqs. (8)–(10), and the different coefficients have the following expressions:

$$\begin{aligned}
&\alpha_h = g'^2[\delta^2_{++} - \delta^2_{-+}], && \alpha^t_{hl} = \frac{g_L^2}{2}G_l^{++}, && \alpha^t_{hq} = \frac{g_L^2}{2}G_q^{++}, && \alpha^s_{hl} = -\frac{g'^2}{2}G_l^{++} + g_R^2 Q_{Z'}(l)G_l^{-+}, \\
&\alpha_{he} = -g'^2 G_e^{++} + g_R^2 Q_{Z'}(e)G_e^{-+}, && \alpha^t_{ll} = g_L^2 G_{ll}^{++}, && \alpha^t_{lq} = g_L^2 G_{lq}^{++}, && \alpha^s_{ll} = \frac{g'^2}{4}G_{ll}^{++} + g_{Z'}^2 Q_{Z'}^2(l)G_{ll}^{-+}, \\
&\alpha^s_{hq} = \frac{g'^2}{6}G_q^{++} + g_R^2 Q_{Z'}(q)G_q^{-+}, && \alpha_{hu} = \frac{2g'^2}{3}G_u^{++} + g_R^2 Q_{Z'}(u)G_u^{-+}, && \alpha_{hd} = -\frac{g'^2}{3}G_d^{++} + g_R^2 Q_{Z'}(d)G_d^{-+}, \\
&\alpha^s_{lq} = -\frac{g'^2}{12}G_{lq}^{++} + g_{Z'}^2 Q_{Z'}(l)Q_{Z'}(q)G_{lq}^{-+}, && \alpha_{le} = \frac{g'^2}{2}G_{le}^{++} + g_{Z'}^2 Q_{Z'}(l)Q_{Z'}(e)G_{le}^{-+}, \\
&\alpha_{qe} = -\frac{g'^2}{6}G_{qe}^{++} + g_{Z'}^2 Q_{Z'}(q)Q_{Z'}(e)G_{qe}^{-+}, && \alpha_{lu} = -\frac{g'^2}{3}G_{lu}^{++} + g_{Z'}^2 Q_{Z'}(l)Q_{Z'}(u)G_{lu}^{-+}, \\
&\alpha_{ld} = \frac{g'^2}{6}G_{ld}^{++} + g_{Z'}^2 Q_{Z'}(l)Q_{Z'}(d)G_{ld}^{-+}, && \alpha_{ee} = g'^2 G_{ee}^{++} + g_{Z'}^2 Q_{Z'}(e)^2 G_{ee}^{-+}, \\
&\alpha_{eu} = -\frac{2g'^2}{3}G_{eu}^{++} + g_{Z'}^2 Q_{Z'}(e)Q_{Z'}(u)G_{eu}^{-+}, && \alpha_{ed} = \frac{g'^2}{3}G_{ed}^{++} + g_{Z'}^2 Q_{Z'}(e)Q_{Z'}(d)G_{ed}^{-+},
\end{aligned} \tag{A24}$$

with $g_L = g_{5L}/\sqrt{L}$, and similarly for the other gauge couplings. Here we use the notation $Q_{Z'}(\psi)$ to denote the charge $Q_{Z'}$ in Eq. (A4) for the fermion ψ.

2. Heavy fermion effects at one loop

The leading effects, due to the KK excitations that mix with the top quark, can be computed using the results in Refs. [19,20]. The one-loop contributions due to quarks to the T and S oblique parameters are

$$\begin{aligned}T = {} & \frac{3}{16\pi s^2 c^2 m_Z^2}\Bigg\{\sum_{i,j}(V^L_{ij}V^{L*}_{ij} + V^R_{ij}V^{R*}_{ij})\theta_+(\mathcal{M}_{ii}, \mathcal{M}_{jj}) \\ & + 2\,\mathrm{Re}(V^L_{ij}V^{R*}_{ij})\theta_-(\mathcal{M}_{ii}, \mathcal{M}_{jj}) \\ & - \sum_i\sum_j^{i-1}(U^L_{ij}U^{L*}_{ij} + U^R_{ij}U^{R*}_{ij})\theta_+(\mathcal{M}_{ii}, \mathcal{M}_{jj}) \\ & + 2\,\mathrm{Re}(U^L_{ij}U^{R*}_{ij})\theta_-(\mathcal{M}_{ii}, \mathcal{M}_{jj})\Bigg\},\end{aligned} \tag{A25}$$

$$\begin{aligned}S = {} & \frac{3}{4\pi}\sum_{i,j}[(U^L_{ij}Y^L_{ji} + U^R_{ij}Y^R_{ji})\bar{\chi}_+(\mathcal{M}_{ii}, \mathcal{M}_{jj}) \\ & + (U^L_{ij}Y^R_{ji} + U^R_{ij}Y^L_{ji})\bar{\chi}_-(\mathcal{M}_{ii}, \mathcal{M}_{jj})],\end{aligned} \tag{A26}$$

where the indices i, j run over all fermions in the theory (SM fermions and their KK excitations),

$$\theta_+(y_1, y_2) = y_1^2 + y_2^2 - \frac{2y_1^2y_2^2}{y_1^2 - y_2^2}\ln\frac{y_1^2}{y_2^2}, \tag{A27}$$

$$\theta_-(y_1, y_2) = 2y_1y_2\left(\frac{2y_1^2y_2^2}{y_1^2 - y_2^2}\ln\frac{y_1^2}{y_2^2} - 2\right), \tag{A28}$$

and

$$\bar{\chi}_+(y_1, y_2) = \frac{5(y_1^4 + y_2^4) - 22y_1^2y_2^2}{9(y_1^2 - y_2^2)^2} + \frac{3y_1^2y_2^2(y_1^2 + y_2^2) - (y_1^6 + y_2^6)}{3(y_1^2 - y_2^2)^3} \ln\left(\frac{y_1^2}{y_2^2}\right) - \frac{2}{3}\ln\left(\frac{y_1y_2}{\mu^2}\right),$$

$$\bar{\chi}_-(y_1, y_2) = \frac{y_1y_2}{(y_1^2 - y_2^2)^3}\left[y_1^4 - y_2^4 - 2y_1^2y_2^2 \ln\left(\frac{y_1^2}{y_2^2}\right)\right]. \quad \text{(A29)}$$

In the above, $\mathcal{M}$ is the (diagonal) mass matrix, containing all fermions in the theory, V^L (V^R) is the matrix of couplings of LH (RH) fermion fields to W_μ^1 in the mass eigenstate basis, and U^L (U^R) is the corresponding matrix of couplings to W_μ^3. The matrices $U^{L,R}$ are Hermitian. Finally, $Y^{L,R}$ are the matrices of hypercharges for left- and right-handed fermions in the mass eigenstate basis.

The leading one-loop contribution to the $Zb_L\bar{b}_L$ coupling, that comes from the quarks with charge $2/3$, reads

$$\delta g_{Zbb} = \frac{\alpha}{2\pi}\left\{\sum_i [V_{ib}^L V_{ib}^L (F_{\rm SM}(r_i) + \tilde{F}(U_{ii}^L/2 - 1/2, U_{ii}^R/2, r_i))] - F_{\rm SM}(r_t) + \sum_{i<j} V_{ib}^L V_{jb}^L \mathcal{F}(U_{ij}^L/2, U_{ij}^R, r_i, r_j)\right\}, \quad \text{(A30)}$$

where $r_i \equiv m_i^2/m_W^2$ and

$$F_{\rm SM}(r) = \frac{1}{8s^2}\frac{r(r-1)(r-6) + r(3r+2)\ln r}{(r-1)^2},$$

$$\tilde{F}(\tilde{g}_L, \tilde{g}_R, r) = \frac{1}{8s^2}\left[r\tilde{g}_L\left(2 - \frac{4}{r-1}\ln r\right) - r\tilde{g}_R\left(\Delta + \frac{2r-5}{r-1} + \frac{r^2-2r+4}{(r-1)^2}\ln r\right)\right],$$

$$\mathcal{F}(\tilde{g}_L, \tilde{g}_R, r, r') = \frac{1}{4s^2(r'-r)}\left\{2\tilde{g}_L\left[\frac{r-1}{r'-1}r'^2\ln r' - \frac{r'-1}{r-1}r^2\ln r\right] - \tilde{g}_R\sqrt{rr'}\left[(\Delta+1)(r'-r) + \frac{r'+4}{r'-1}r'\ln r' - \frac{r+4}{r-1}r\ln r\right]\right\}. \quad \text{(A31)}$$

[1] L. Randall and R. Sundrum, Phys. Rev. Lett. **83**, 3370 (1999).
[2] Y. Grossman and M. Neubert, Phys. Lett. B **474**, 361 (2000).
[3] T. Gherghetta and A. Pomarol, Nucl. Phys. **B586**, 141 (2000); S. J. Huber and Q. Shafi, Phys. Lett. B **498**, 256 (2001).
[4] M. E. Peskin and T. Takeuchi, Phys. Rev. D **46**, 381 (1992).
[5] K. Agashe, A. Delgado, M. J. May, and R. Sundrum, J. High Energy Phys. 08 (2003) 050.
[6] K. Agashe, R. Contino, L. Da Rold, and A. Pomarol, Phys. Lett. B **641**, 62 (2006).
[7] A. Djouadi, G. Moreau, and F. Richard, Nucl. Phys. **B773**, 43 (2007).
[8] M. Carena, E. Pontón, J. Santiago, and C. E. M. Wagner, Nucl. Phys. **B759**, 202 (2006).
[9] G. Cacciapaglia, C. Csaki, C. Grojean, and J. Terning, Phys. Rev. D **71**, 035015 (2005).
[10] N. S. Manton, Nucl. Phys. **B158**, 141 (1979); Y. Hosotani, Phys. Lett. **126B**, 309 (1983); H. Hatanaka, T. Inami, and C. S. Lim, Mod. Phys. Lett. A **13**, 2601 (1998); I. Antoniadis, K. Benakli, and M. Quiros, New J. Phys. **3**, 20 (2001); M. Kubo, C. S. Lim, and H. Yamashita, Mod. Phys. Lett. A **17**, 2249 (2002); G. von Gersdorff, N. Irges, and M. Quiros, Nucl. Phys. **B635**, 127 (2002); C. Csaki, C. Grojean, and H. Murayama, Phys. Rev. D **67**, 085012 (2003); N. Haba, M. Harada, Y. Hosotani, and Y. Kawamura, Nucl. Phys. **B657**, 169 (2003); **B669**, 381(E) (2003); C. A. Scrucca, M. Serone, and L. Silvestrini, Nucl. Phys. **B669**, 128 (2003); C. A. Scrucca, M. Serone, L. Silvestrini, and A. Wulzer, J. High Energy Phys. 02 (2004) 049; N. Haba, Y. Hosotani, Y. Kawamura, and T. Yamashita, Phys. Rev. D **70**, 015010 (2004); C. Biggio and M. Quiros, Nucl. Phys. **B703**, 199 (2004); Y. Hosotani, S. Noda, and K. Takenaga, Phys. Lett. B **607**, 276 (2005); G. Cacciapaglia, C. Csaki, and S. C. Park, J. High Energy Phys. 03 (2006) 099; G. Panico, M. Serone, and A. Wulzer, Nucl. Phys. **B739**, 186 (2006); **B762**, 189 (2007); A. Falkowski, Phys. Rev. D **75**, 025017 (2007).
[11] R. Contino, Y. Nomura, and A. Pomarol, Nucl. Phys. **B671**, 148 (2003).
[12] K. Agashe, R. Contino, and A. Pomarol, Nucl. Phys. **B719**, 165 (2005); K. Agashe and R. Contino, Nucl. Phys. **B742**, 59 (2006).
[13] G. Cacciapaglia, C. Csaki, G. Marandella, and J. Terning, Phys. Rev. D **75**, 015003 (2007).
[14] W. Buchmuller and D. Wyler, Nucl. Phys. **B268**, 621 (1986).
[15] Z. Han and W. Skiba, Phys. Rev. D **71**, 075009 (2005); Z. Han, Phys. Rev. D **73**, 015005 (2006).
[16] F. del Aguila, M. Perez-Victoria, and J. Santiago, Phys.

Lett. B 492, 98 (2000); J. High Energy Phys. 09 (2000) 011.
[17] F. del Aguila and J. Santiago, Phys. Lett. B **493**, 175 (2000); arXiv:hep-ph/0011143.
[18] F. Del Aguila and J. Santiago, J. High Energy Phys. 03 (2002) 010.
[19] L. Lavoura and J. P. Silva, Phys. Rev. D **47**, 2046 (1993).
[20] P. Bamert, C. P. Burgess, J. M. Cline, D. London, and E. Nardi, Phys. Rev. D **54**, 4275 (1996).
[21] A. Manohar and H. Georgi, Nucl. Phys. **B234**, 189 (1984); M. A. Luty, Phys. Rev. D **57**, 1531 (1998); A. G. Cohen, D. B. Kaplan, and A. E. Nelson, Phys. Lett. B **412**, 301 (1997).
[22] Z. Chacko, M. A. Luty, and E. Pontón, J. High Energy Phys. 07 (2000) 036.
[23] W. M. Yao *et al.* (Particle Data Group), J. Phys. G **33**, 1 (2006).
[24] J. Hirn and V. Sanz, Phys. Rev. Lett. **97**, 121803 (2006); J. High Energy Phys. 03 (2007) 100.
[25] K. Agashe, A. Belyaev, T. Krupovnickas, G. Perez, and J. Virzi, arXiv:hep-ph/0612015.
[26] K. Agashe and G. Servant, J. Cosmol. Astropart. Phys. 02 (2005) 002.
[27] K. Agashe, G. Perez, and A. Soni, Phys. Rev. D **75**, 015002 (2007).
[28] P. M. Aquino, G. Burdman, and O. J. P. Eboli, Phys. Rev. Lett. **98**, 131601 (2007).
[29] CDF Collaboration, "*Search for Heavy Top* $t' \rightarrow Wq$ *in Lepton Plus Jets Events*" Report No. CDF-note-8495; J. Conway (private communication).
[30] T. Aaltonen *et al.* (CDF Collaboration),arXiv:0706.3264.
[31] M. Carena and H. E. Haber, Prog. Part. Nucl. Phys. **50**, 63 (2003).
[32] J. A. Aguilar-Saavedra, Phys. Lett. B **625**, 234 (2005); **633**, 792(E) (2006); Proc. Sci., TOP2006 (2006) 003 [arXiv:hep-ph/0603199].
[33] D. Costanzo, Report No. ATL-PHYS-2004-004; G. Azuelos *et al.*, Eur. Phys. J. C **39S2**, 13 (2005).
[34] J. A. Aguilar-Saavedra, J. High Energy Phys. 12 (2006) 033.
[35] G. Cacciapaglia, C. Csaki, G. Marandella, and J. Terning, J. High Energy Phys. 02 (2007) 036.
[36] R. Contino, L. Da Rold, and A. Pomarol, Phys. Rev. D **75**, 055014 (2007).